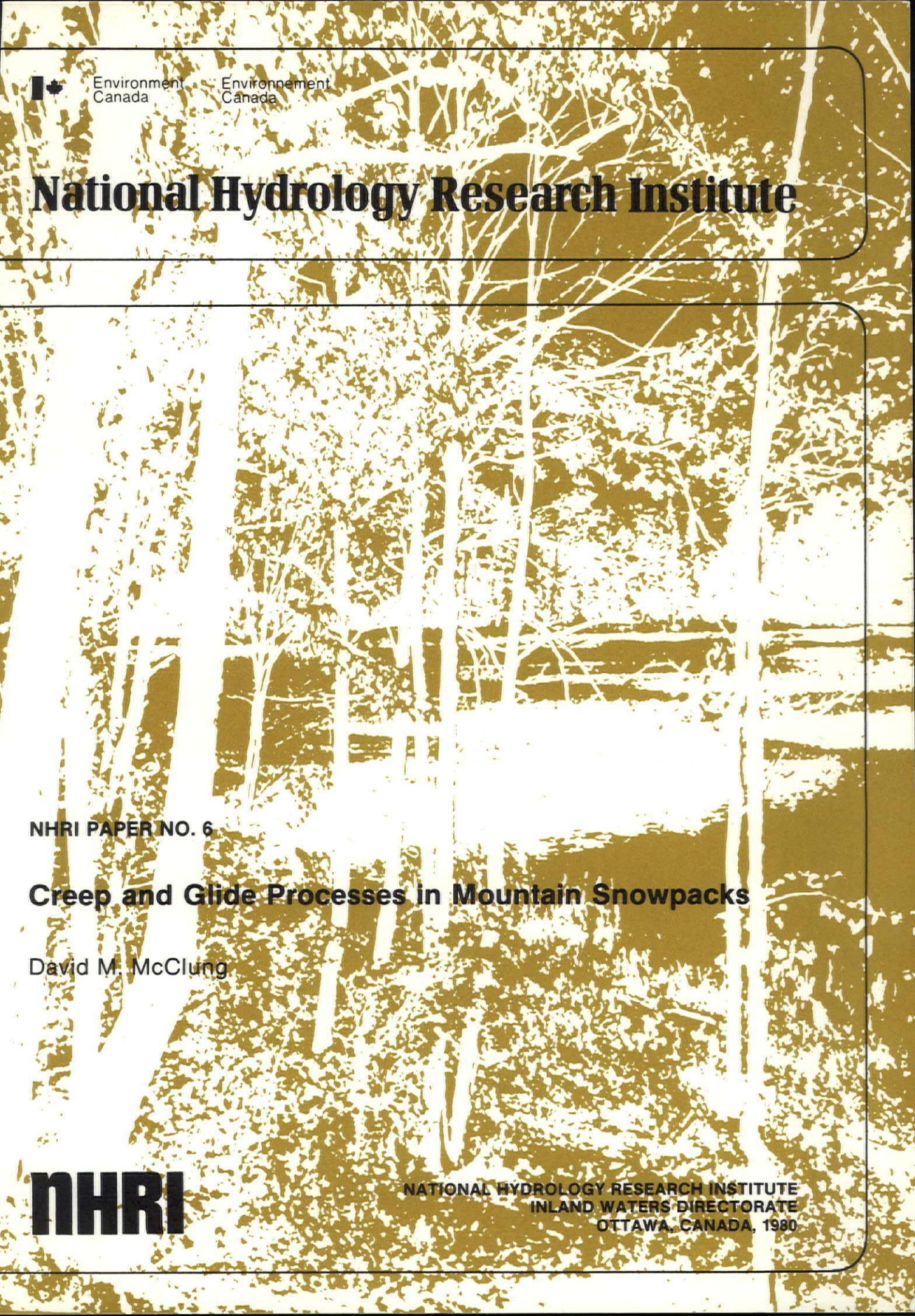

Environment Canada Environnement Canada

National Hydrology Research Institute

NHRI PAPER NO. 6

Creep and Glide Processes in Mountain Snowpacks

David M. McClung

NHRI

NATIONAL HYDROLOGY RESEARCH INSTITUTE
INLAND WATERS DIRECTORATE
OTTAWA, CANADA, 1980

Environment Canada Environnement Canada

National Hydrology Research Institute

NHRI PAPER NO. 6

Creep and Glide Processes in Mountain Snowpacks

David M. McClung

NHRI

NATIONAL HYDROLOGY RESEARCH INSTITUTE
INLAND WATERS DIRECTORATE
OTTAWA, CANADA, 1980

Contents

Table

Illustrations

Abstract

Creep and glide processes in mountain snowpacks are discussed from the point of view of relevant constitutive equations for internal deformation (creep) in the material and slip boundary conditions (glide) at the base of slabs or the entire snowpack. The emphasis on the creep equations is to attain a formulation which is easily applicable in problems and which matches the known characteristics of field data rather than the most general equation. For glide, constitutive equations relating drag shear stress, τ, to slip velocity are given for three mechanisms for neutral zone conditions and a step toward the formulation of a general theory of snow gliding is made. Non-neutral zone glide boundary conditions are also introduced, and these are related to release of full depth and wet slab avalanches and to the problem of snow pressure on avalanche defence structures. Porous media effects on glide are also discussed.

Résumé

Le présent ouvrage traite de la question du cheminement et du glissement des neiges, en vue de formuler des équations constitutives pertinentes pour exprimer la déformation interne (cheminement) du matériau et les conditions limites de glissement (planage) au pied des pans de neige ou de toute la couverture de neige. En établissant les équations de cheminement pour remplacer les équations plus générales, on cherche une formule d'application facile qui va permettre de résoudre les problèmes concrets et bien refléter la réalité observée sur le terrain. Pour le glissement, on présente des équations constitutives montrant le rapport entre le travail au cisaillement dû au tirage, τ, et la vitesse de glissement, pour trois mécanismes, en zone neutre, et on ouvre la voie à la formulation d'une théorie générale du glissement de la neige ou planage. On y présente, entre autres, les conditions limites de glissement en zone non neutre et le rapport entre celles-ci et le déclenchement des avalanches, qu'il s'agisse de toute la couverture ou de pans mouillés, ou encore le problème de la pression exercée par la neige sur les ouvrages de protection contre les avalanches. De plus, il y est question de l'influence des matériaux poreux sur le planage.

Introduction

Creep is defined as the slow, viscous internal deformation in snowpacks, and glide, as the slip of the entire snowpack over the ground or of a snow slab over an internal layer within the snowpack. Understanding the physics of these processes is of the utmost importance in formulating the constitutive relations necessary to solve practical problems such as calculation of snow pressures on structures as well as in understanding the important problem of the mechanism of release of wet slab avalanches and full depth slab avalanches.

In this report, approximate constitutive equations relating stresses to viscous strain-rates are discussed which are consistent with data taken from field experiments. In particular, a simple two-parameter equation is discussed which may be applicable in practical problems. For glide, constitutive relations are given relating shear stress to the glide velocity at the glide interface for three physical mechanisms of glide, and a general theory of gliding is outlined incorporating these three mechanisms. Following these treatments, two important applications are developed for the case in which there is a gradient in glide conditions at the interface.

Creep in Mountain Snowpacks

The characteristics of viscous creep in the seasonal alpine snowpack are important in formulating steady glide constitutive equations and viscous constitutive equations to describe internal deformation in alpine snow. Undoubtedly, formulation of accurate non-linear viscous constitutive equations that are valid in general is a formidable task. In this report we only speculate on the aspects of the problem which are accessible from field measurements. We consider the class of viscous constitutive equations for which creep velocity gradients are small but in which non-linearity is permitted. Our goal is to explore forms of the constitutive equations useable for plane problems and consistent with field measurements. We seek to develop equations which are plausible and applicable rather than the most general equations possible. A general constitutive equation is likely to be very complex (Salm, 1967; 1975) and would evidently have very little practical use if it could be written.

CONSTITUTIVE RELATIONS FROM NEUTRAL ZONE CREEP MEASUREMENTS

Field data are potentially very important in formulating constitutive equations because they indicate conditions that are natural and difficult to reproduce in a laboratory experiment. Experiments that involve slow, viscous creep are of particular interest because they are relevant to the important problems of snow pressure and steady glide constitutive equations.

The usual approach for such experiments is the classic method pioneered by Haefeli of taking a core out of the snowpack and back filling with a deformable material such as sawdust after placing height markers in the column. Using this method in the neutral zone, information can be obtained about both components of creep deformation, and the shear and vertical strain-rates can be extracted.

Analysis of data for *well-settled* alpine snow on open slopes shows that the components of creep deformation in the neutral zone are approximately linear with depth. There are, however, some important considerations before these results can be interpreted in terms of a constitutive theory. Figure 1a depicts a scheme of typical neutral zone data. McClung (1974) gives a detailed discussion of the experiments and data.

It is evident that creep in the seasonal alpine snowpack is never steady state. In steady-state creep theory if the stress, σ, is constant the rate of creep deformation

is also constant. It is clearly evident that this is not the case here. In a seasonal alpine snowpack there is extensive bulk deformation which densifies the snow, so that the rate of creep deformation is a function of not only stress but also time. Snow is inherently unstable, as its structure and properties change on prolonged exposure to any temperature even without load.

Consider the deformation profile in the neutral zone. In this case, the ratio of shear stress, τ, to normal stress, σ, is constant. On the other hand, the shear strain-rate, $\dot{\gamma}$, is approximately independent of depth at any instant of time but will logically decrease with time as densification proceeds. In accord with these results we are tempted to write:

$$\dot{\gamma} = K\frac{\tau}{\sigma} \tag{1}$$

at any instant in time where $K = K(\rho, T, St)$ depends on density (ρ), temperature (T), and snow structure (St) at any instant of time but decreases slowly with time as densification proceeds. Thus, as time passes, $\dot{\gamma}$ and K decrease slowly, while the ratio τ/σ remains independent of time.

Another way to explain the neutral zone deformation profile might be via a linear relationship between $\dot{\gamma}$ and τ at any instant of time with K a sensitive function of ρ, T or St. Field measurements, however, argue against this approach because the shear deformation profile is quite straight, whereas the density, for example, increases with depth but scatters considerably. The proportionality between shear strain-rate and τ appears from field data to be a density-integrated stress-dependent effect.

Field data also show that the vertical strain-rate, $\dot{\varepsilon}$, is approximately independent of depth at any instant of time. This may be expressed as:

$$\dot{\varepsilon} = -\beta\dot{\gamma} \tag{2}$$

where β is constant at any instant of time but should decrease with time as the snowpack densifies.

With the identifications $\dot{\gamma} = (\frac{1}{2}\dot{e}_{ij}'\dot{e}_{ij}')^{\frac{1}{2}}$, $\dot{\varepsilon} = \dot{e}_{kk}$ and $\bar{\tau} = (\frac{1}{2}\sigma_{ij}'\sigma_{ij}')^{\frac{1}{2}}$, $\bar{\sigma} = -\frac{1}{3}\sigma_{kk}$ (where a prime denotes the deviatoric part of a tensor), Equations 1 and 2 can be generalized to arbitrary stress states:

$$\dot{e}_{ij}' = \left(\frac{K}{\bar{\sigma}}\right)\sigma_{ij}' \tag{3}$$

$$\dot{e}_{kk} = - \frac{\beta K \bar{\tau}}{\bar{\sigma}} \tag{4}$$

With $\sigma_{ij}' = \sigma_{ij} - \frac{1}{3} \sigma_{kk} \delta_{ij}$, these equations may be expressed as:

$$\sigma_{ij} = \frac{\bar{\sigma}}{K} \dot{e}_{ij} - \delta_{ij} \left(K + \frac{1}{3} \dot{e}_{kk}\right) \frac{\bar{\sigma}}{K} \tag{5}$$

This permits definition of effective moduli analogous to shear and bulk viscosity:

$$\bar{\mu} = \frac{\bar{\sigma}}{2K} \quad ; \quad \bar{\eta} = - \frac{\bar{\sigma}}{\dot{\bar{\varepsilon}}} \tag{6}$$

which are proportional to the mean stress, $-\bar{\sigma}$. The effective viscous analog of Poisson's ratio could be expressed:

$$\bar{\nu} = \frac{1}{2} \left[\frac{3 - 2\left(\frac{\dot{\bar{\varepsilon}}}{K}\right)}{3 + \left(\frac{\dot{\bar{\varepsilon}}}{2K}\right)} \right] \tag{7}$$

Equations 6 and 7 predict approximately linear shear and bulk viscosity with depth at any instant of time and viscous Poisson ratio independent of depth with all three of these quantities slowly increasing with time.

Field measurements are far more numerous than laboratory measurements in providing verification for such a formulation. The sawdust column experiments of McClung (1974) from the deep, dense maritime snow cover of the Cascade Mountains in the United States provided shear strain-rates which are consistently lower than the reported results in shallower (and presumably less dense) snow covers in Switzerland and Colorado. In addition, experiments by McClung (1974) measuring the tilt of poles of various lengths on the same slope with a sensitive inclinometer showed that the tilt-rate of the poles was approximately independent of length, indicating again that the shear strain-rate is approximately independent of depth provided the snow is very well settled. Haefeli (Bader *et al.*, 1939) provided laboratory data which showed that the shear strain-rate is proportional to τ/σ for fairly dense snow, but the small number of data he gave do not permit any general conclusion.

Another point is that an equation like Equation 1 has a definite frictional character and cannot be expected to apply for stress states like pure shear where the ratio $\bar{\tau}/\bar{\sigma}$ is undefined. This shortcoming may not, however, detract from the usefulness of such equations for quasi-static calculations in snowpack problems. Certainly, there is no generality in the argument presented here, but the argument does provide a framework for investigation of bulk stress effects in snow pressure problems. McClung (1976a) used similar equations for calculations of snow pressure for the plane strain-rate problem at the middle of an avalanche defence structure. The results show that bulk stress effects can increase snow pressures by a factor of approximately 20%.

Pressure dependence of moduli is a persistent result in stress-deformation measurements for granular materials. Domaschuk and Wade (1969) showed that the initial small deformation shear and bulk moduli are linear functions of pressure for sand. Wroth (1972) showed that a similar relationship applies for over-consolidated clay. Such a relationship is also consistent with results on dry snow. Figure 2 shows the small deformation shear modulus for five similar snow samples sheared at the same rate for different values of normal stress in simple shear from experiments by the present author. A relationship for which the viscosity is constant at zero pressure, as Figure 2 indicates, would also remove the objection to inapplicability of the formalism to pure shear stress states while still retaining approximate agreement with neutral zone results, although it results in a more complex formalism.

Glide in Mountain Snowpacks

Glide is defined as the slow, steady slip of a snow slab over a wetted interface within the snowpack, such as an ice layer, or over the ground. Field experiments indicate that for glide to occur at the snow-earth interface, water must be present. Water, of course, serves as a lubricant to initiate and maintain glide.

In this report snow gliding theory is discussed in terms of two conditions at the glide interface: (1) the snowpack conforms to the interface over which it is gliding (no separation) and (2) the snowpack is physically separated from the glide interface by a thin (but not infinitesimally thin) water film. This division simplifies discussion of the theoretical aspects of the problem; however, it should be recognized that in realistic field situations such a division cannot easily be made.

Inertial forces are negligible for the slow, steady slip described in this paper. When there is no separation, the resistance to motion is due to the deformation which the snow undergoes in conforming to the shape of the glide interface and also possibly from regelation whereby the snow may melt under pressure on the uphill side of asperities at the glide interface and refreeze on the downhill sides. Glide constitutive equations for these processes are given relating the average drag shear stress $\langle \tau_{xz} \rangle$ at the glide interface to the glide velocity U_0. Although the evidence is far from conclusive, it seems likely that the role of regelation is very minor in most field situations; this point is further discussed in Chapter 3.

When the slope angle is high enough and the roughness of the glide surface is low enough, separation of the snowpack or snow slab from the glide interface is possible at local points along the surface. If this were to happen, regelation and deformation around asperities would not be possible. For a water film thickness which is thin enough, however, steady glide is still possible in which the drag is provided by the viscosity of the water in the fluid layer in interaction with the geometry of the asperities at the glide interface and the snow slab sliding over the asperities. Steady glide, however, is only possible when the thickness of the water layer is small. Then, there may be significant drag due to a large rate of strain and viscous stress. As the water layer becomes thicker, the drag drops rapidly to zero, resulting in instability.

In this report, the conditions under which separation is bound to occur are described, and the general form of the constitutive relations relating the average drag

shear stress to the glide velocity is given for steady glide. This mechanism of glide will be termed the "lubrication sliding mechanism."

The three glide mechanisms and their constitutive equations form the basis for a general theory of steady glide under conditions in which there is no gradient in large-scale[1] roughness features, water content or stress conditions along the gliding interface. The conditions prior to wet slab avalanche release, however, require a gradient in glide conditions at the interface. This may be due to the presence of varying amounts of water at the interface and/or variations in the interface geometry. These conditions may, under certain circumstances, induce a changing relationship between the drag $\langle \tau_{xz} \rangle$ and the glide velocity at the interface analogous to plasticity relationships seen in yielding of geotechnical materials. It is possible under the appropriate conditions, for example, for the relationship between $\langle \tau_{xz} \rangle$ and U_0 to parallel that of strain-softening seen in the failure of geotechnical materials. Such a process will generate high tensile stresses in the slab, making tensile fractures possible depending on boundary condition at the glide interface.

MECHANISMS OF STEADY GLIDE AND THEIR CONSTITUTIVE RELATIONS FOR THE CASE OF NO SEPARATION

Glide by Creep

When the snowpack conforms to a wetted glide interface, two possible mechanisms of steady glide are: (1) creep over asperities at the interface and (2) motion by regelation, that is, pressure melting of snow on the upstream sides and possible refreezing on the downstream side or some related process. In theory, these mechanisms may compete when the snow slab does not separate from the glide interface.

We consider first the case of creep of a snow slab over a general boundary, with the interface surface represented as $z = Z_0(x,y)$ and the snow slab and interface inclined at an angle Ψ to the horizontal (Fig. 1b). We seek a relationship between the drag shear stress $\langle \tau_{xz} \rangle$, which shall henceforth be written as τ, at the base of the slab and the interface glide velocity.

To simplify the mathematics, the snow is modelled as an incompressible Newtonian fluid flowing at velocities slow enough so that inertial effects may be disregarded. The velocity field, $\vec{u}\,(x,y,z) = (u\hat{e}_x, v\hat{e}_y, w\hat{e}_z)$, then satisfies the equation:

[1] Large scale here means much larger than the scale of the asperities at the glide interface.

$$\mu\nabla^2\vec{u} - \nabla P = 0 \tag{8}$$

where $P(x,y,z)$ is the mean pressure and μ is the viscosity of the snow. Since the flow is assumed to be incompressible,

$$\nabla\cdot\vec{u} = 0 \tag{9}$$

We seek solutions to these equations consistent with the boundary conditions of the problem in the limit for low roughness, which are:

(1) $\vec{u} \to U_0\hat{e}_x$ far away from the boundary,

(2) $\vec{u}$ is tangential to $Z_0(x,y)$ at the interface, and

(3) the shear stress parallel to $Z_0(x,y)$ is zero.

When the snow conforms to the glide interface, the vertical component of the velocity, w, must be given by

$$w = U_0 \frac{\partial Z_0}{\partial x} \tag{10}$$

Similarly, the lateral component of velocity v is given by $v = 0$ in the low bed roughness limit (Kamb, 1970), where roughness means ratio of amplitude to wavelength.

The condition that the shear stress vanish at the glide interface is required because the interface is wet and, therefore, a shear stress cannot be supported. The condition that the interface be free from shear stress is equivalent to the condition that $u = U_0$ there (Kamb, 1970). These last conditions are true in the limit by constraining the snow to conform to the interface in the limit approaching a smooth interface of low roughness.

Under the constraints stated above, the principal boundary conditions are in terms of $\vec{u}$ alone. In this case, the solution to the problem reduces to the solution of:

$$\nabla^2(\nabla\times\vec{u}) = 0 \quad , \quad \nabla\cdot\vec{u} = 0 \tag{11}$$

with the pressure then calculated by Equation 8.

The general form of the solution to these equations (Batchelor, 1967) is:

$$\vec{u} = U_0 \cdot \left[\text{function } \left(\frac{\vec{x}}{L}, \text{ geometry of boundary conditions}\right)\right]$$

$$P - P_0 = \frac{\mu U_0}{L} \cdot \left[\text{function } \left(\frac{\vec{x}}{L}, \text{ geometry of boundary conditions}\right)\right] \tag{12}$$

where L is a relevant length scale for the problem and P_0 is a reference pressure.

For the present problem, since there is no boundary shear stress, the equivalent drag shear stress is the downslope component of the boundary normal stress, $\sigma_{zz}(x,y,0)$. The boundary normal stress may be calculated from the assumed linear constitutive equation:

$$\sigma_{ij} = 2\mu\dot{e}_{ij} - \delta_{ij}P$$

Now on the boundary, $\dot{e}_{zz} = \frac{\partial w}{\partial z}$ is given by

$$\frac{\partial w}{\partial z} = U_0 \frac{\partial^2 Z_0}{\partial x \partial z} = 0 \tag{13}$$

and therefore,

$$\sigma_{zz}(x,y,0) = -P(x,y,0)$$

so that $P(x,y,0)$ represents the interface film pressure.

Thus, we can write, in general,

$$\sigma_{zz}(x,y,0) = -\frac{\mu}{L} U_0 \cdot \left[\text{function}\left(\frac{\vec{x} = x,y,0}{L}\right), \text{ geometry of boundary conditions}\right] \tag{14}$$

We seek now the relationship between the average basal shear stress and the glide velocity. Following Kamb (1970), the average basal shear stress is defined as the average of the x component of σ_{zz} on the surface $Z_0(x,y)$,

$$\tau = \langle \tau_{xz} \rangle = \frac{1}{S} \int_{Z=Z_0} \sigma_{zz}(x,y,0)\hat{e}_x \cdot d\vec{s} = -\frac{1}{S} \int_{Z=Z_0} P(x,y,0)\hat{e}_x \cdot d\vec{s} \qquad (15)$$

where $\hat{e}_x$ is a unit vector in the x direction and $d\vec{s}$ is a surface element with direction normal to the surface, S. This equation may be rewritten:

$$\tau = \left\langle P(x,y,0) \frac{\partial Z_0}{\partial x} \right\rangle \qquad (16)$$

Therefore, the general form of the glide constitutive equation is:

$$\tau = \frac{\mu U_0}{L} \cdot \text{(function of geometry)} \qquad (17)$$

For the general case, this equation may be expressed in the form:

$$\tau = \frac{\mu U_0}{D} \qquad (18)$$

where D is a field measurable parameter called a stagnation depth which is a function only of the geometry of the boundary conditions suitably averaged along the glide interface. The parameter D represents the missing length scale in the problem whose simple geometric interpretation is well known (Fig. 1b) (Nye, 1969; McClung, 1975). Kamb (1970) gave calculations from which D could be extracted by Fourier analysis of the interface in terms of the distribution of a roughness function, r, an index of which is the ratio of amplitude to wavelength for any Fourier component.

There are many existing detailed calculations of D. Kamb (1970) gives D, for example, for the following spectral distributions of r: (1) white roughness ($|r|$ constant); (2) truncated white roughness ($|r|$ constant for all wavelengths below a fixed lower limit); (3) single wavelength and (4) cross-corrugated sinusoidal waves.

Field measurements of D (McClung, 1975; Salm, 1977) indicate that it varies from D = 0, for the case in which there is no water present at the glide interface, up to about D = 3H where H is the depth of the pack perpendicular to the glide interface.

Glide by Regelation

It may be possible for steady glide to occur by regelation, since snow is composed of a matrix of ice grains and ice can melt under pressure. The essence of the phenomena, as it is usually discussed for the similar problem in glacier sliding, is that melting occurs at the high-pressure upstream sides of asperities and this is followed by refreezing on the downstream sides. There are, however, some indications that regelation

plays a minor if not negligible role in the snow gliding process. First, typical depths of the alpine snow cover usually mean that the pressures at the glide interface are much lower than those at the base of a glacier where the process is known to occur. Secondly, there is some experimental evidence that glide does not occur on slopes such as rock faces where small wavelength asperities are present unless there is a good amount of water. If one compares the solution for glide regelation with that for creep, for the single sine wave case, one finds that it is not possible for glide to occur by creep over small wavelength asperities, although glide should be easy over the small wavelength asperities if regelation is taking place. Glide observations on rock slopes in western Norway (McClung, 1976b) and in Switzerland (Salm, personal communication) indicate that glide occurs only when a large quantity of water is present at the interface. This could be taken to mean that the small wavelength asperities had to be drowned before glide could occur, although the meagre evidence to date is far from conclusive. Since the snow at the glide interface is at the melting point when glide occurs, there is undoubtedly regelation in some form taking place as the grains move by each other and over the asperities; yet the role of the process in the creep mechanism or by itself as a viable glide mechanism is not well understood. Quantitative evaluation of the process as a glide mechanism will be hampered until the basic physics is understood and until careful regelation experiments are performed on snow to permit a satisfactory definition of the relationship between the pressure at the glide interface and the melting point temperature.

Like the glide constitutive equation for creep over asperities, the corresponding relation for glide by regelation is well known. The general form of the equation is (Kamb, 1970; Nye, 1969, 1970):

$$\tau = K \cdot G \cdot U_0 \tag{19}$$

where K depends on the physical regelation constants and constants of the snow and the glide interface material, and G depends on the geometry of the boundary conditions. Again, several calculations of the product K·G are available in the literature (Nye, 1969, 1970; Kamb, 1970).

Following Nye (1969), this last equation can be rewritten as:

$$\tau = \frac{\mu U_0}{D_R} \tag{20}$$

where $D_R = \mu / K \cdot G$ to get a form analogous to Equation 18 for the creep solution.

To discuss creep and regelation as competing mechanisms the superposition rule outlined by Nye (1969) must be used. The connecting link between the creep and regelation

mechanisms is the pressure in the water film at the glide interface. Only in the case of a boundary of a single sinusoid does the pressure for the two solutions have the same form. Therefore Nye's superposition rule states that for a general interface, the interface is decomposed into harmonics, and then for each harmonic, the velocity for pure regelation is added to that for viscous creep. The summation for each harmonic then gives the total velocity produced for a given applied shear stress and the drag produced for a given velocity. For a single sine wave, the forms of the creep and regelation constitutive equations are (e.g., Nye, 1969):

$$\tau = \frac{\mu r^2 (2\pi)^3}{\lambda} U_{0c} \tag{21}$$

and

$$\tau = \frac{L \cdot \lambda \cdot r}{4CK} (2\pi) U_{0R} \tag{22}$$

respectively, where $r = A/\lambda$, the ratio of asperity amplitude to wavelength.

These equations exhibit the expected relationship that for short wavelengths the drag is very high for the creep process, while for long wavelengths the drag is very high for the regelation process. As yet undetermined, C is a constant for snow from the Clausius-Clapeyron equation. The relevant thermal conductivity is K and the latent heat of fusion is L in the problem.

For the ith harmonic, the velocity is then

$$U_{0i} = U_{0ci} + U_{0Ri} = \frac{\lambda i}{\mu r_i^2} \frac{\tau}{(2\pi)^3} + \frac{4CK\tau}{L\lambda_i r_i^2 (2\pi)} \tag{23}$$

or

$$U_{0i} = \left(\frac{D_{ci} + D_{Ri}}{\mu} \right) \tau = \frac{D_i}{\mu} \tau \tag{24}$$

Summing over i, with $U_0 = \sum_i U_i$, $D = \Sigma D_i$, gives

$$U_0 = \frac{D}{\mu} \tau \tag{25}$$

Now D is a measurable parameter and we note that *in cases in which it is expected that creep and regelation will be competing*, if D is much less than the snowpack depth it is expected that the glide process will be mostly by creep. For cases in which D is considerably greater than the snowpack depth, we anticipate that glide will be mostly by regelation. When D is on the order of the snowpack depth, we expect that the processes will be competing equally. As noted, stagnation depths in the range of from near zero up

to 3H have apparently been measured. Nevertheless, this does not mean that regelation is a glide mechanism because the possibility that fast glide may be due to separation effects and large amounts of water is much more likely.

SEPARATION--THE LUBRICATION SLIDING MECHANISM

The fastest measurements of gliding are from smooth slopes covered by grass or smooth rock slopes when appreciable water is present at the glide interface. Measurements of steady glide in Switzerland indicate stagnation depths as high as three times the snow depth (Salm, 1977). This observation, along with the doubtful participation of regelation sliding to any great degree, points to another glide mechanism which may be very important. The mechanism is rigid body sliding of the snowpack over the ground with the snowpack separated from the ground by a thin water film. It cannot occur unless there is physical separation of the snow cover from the asperities over which it may be creeping. This mechanism of glide lubrication will be called sliding. The sliding resistance in this case is provided by viscous resistance in the thin water film. It should be emphasized that the water film must be very thin for this mechanism to produce steady glide because if the water film were thick compared with, for example, asperity amplitudes, the resistance to sliding would become very small and instability would result.

Field measurements consistently indicate that the values of glide velocity show large fluctuations especially when rainfall or excessive melt is taking place. Since both the creep and regelation mechanisms predict a unique glide velocity for a given set of geometry and stress conditions, it seems likely that another mechanism is responsible for those fluctuations, and from the standpoint of the present theory, the fluctuations are attributable to the onset of local separation. In this sense glide would not be steady. However, if a constant water content at the glide interface could be maintained, steady glide would be possible.

It is difficult to understand quantitatively the intermediate steps in which a snowpack undergoing steady creep separates at various points and then subsequently glides mostly by the lubrication sliding mechanism. It is possible, however, to identify the condition under which separation should begin to appear. To do this it should be remembered that the normal pressure on the glide interface can be considered to fluctuate about a mean value set by the overburden pressure for a snowpack where steady glide is mostly by the creep mechanism.

Physically the drag due to creep occurs because the normal pressure on the upstream sides of asperities is greater than on the downstream sides. Since the fluctuations in normal pressure (pressure of the snowpack against the glide interface) can take positive (upstream side) and negative (downstream side) values, it is possible that the fluctuations can be larger than the overburden normal stress, resulting in no pressure of the

snowpack against the glide interface upon which time separation will begin to occur. The fluctuations are large for very smooth glide surfaces where the ratio of amplitude to wavelength is small. Therefore, we expect separation to begin at the downstream sides of asperities on smooth glide interfaces and for cases where the snowpack is thin. Once separation begins it is easier for any water present to flow into the low pressure separation area, thereby leading to increased lubrication and a smaller area of the snowpack in contact with the glide interface leading to faster sliding and perhaps a self-perpetuation of the process.

To investigate the condition for separation, we wish to know when the normal pressure fluctuations begin to approach the overburden pressure. We follow the treatment of Kamb (1970) in our development here.

An index of the normal stress fluctuations is $\langle P^2 \rangle^{\frac{1}{2}}$ for the Fourier-analyzed interface and this is to be compared with the overburden pressure, $\sigma = \rho g H \cos \Psi$.

The equivalent bed shear stress, τ, is given by

$$\tau = \left\langle P \frac{\partial Z_0}{\partial x} \right\rangle \tag{26}$$

For a sinusoidal roughness of a single wavelength, the ratio of $\langle P^2 \rangle^{\frac{1}{2}}/\tau$ is given by:

$$\frac{\langle P^2 \rangle^{\frac{1}{2}}}{\tau} = \frac{\langle P^2 \rangle^{\frac{1}{2}}}{\left\langle \frac{2\pi P}{\lambda} Z_0 \right\rangle} \tag{27}$$

This may be expressed as (Kamb, 1970):

$$\frac{\langle P^2 \rangle^{\frac{1}{2}}}{\tau} = \frac{1}{\pi r \sqrt{2}} \tag{28}$$

where $r = \frac{A}{\lambda}$. This equation defines a quantity like the inverse of a coefficient of friction which is proportional to the roughness parameter r.

As Kamb points out, the actual maximum value of $|P|$ is given by $\langle 2P^2 \rangle$.

In the neutral zone for steady glide, the ratio of $\tau/\sigma = \tan \Psi$, where Ψ is the slope angle. Therefore, the separation condition is approximately:

$$\frac{\langle 2P^2 \rangle^{\frac{1}{2}}}{\sigma} = \frac{2}{\pi\sqrt{2}} \frac{\tan \Psi}{r} \rightarrow 1 \qquad (29)$$

Separation is expected to begin on steep slopes where the roughness parameter is small and also when the overburden normal stress σ is small (thin snowpacks).

Similar relationships could be formulated in the manner of that by Kamb (1970) for more general roughness spectra, but for the case of a linear Newtonian viscous rheology, the results would be little affected over a wide range of values of r (Kamb, 1970). Thus, the general conclusion is that separation is expected on steep slopes for beds of low roughness and thin snowpacks. This result is very much in agreement with field measurements and observations of gliding behaviour. Glide fluctuations are greatest on steep slopes with smooth interfaces early in the season when the snowpack is thin (McClung, 1974).

HAEFELI'S SLIDING BLOCK EXPERIMENTS

Haefeli (Bader *et al.*, 1939) performed experiments which have some relevance to experimental simulation of the lubrication sliding mechanism. He measured the sliding characteristics of snow blocks on glass plates. The experiments were conducted for various interface temperatures and normal stresses. Figure 3 shows an example of Haefeli's data for a dry glass plate, a partially wet interface ($T_i \simeq 0°C$) and a wet interface ($T_i > 0°C$). These data show in general a linear relationship between τ and U_0 and a decrease in the ratio of τ/U_0 with an increasing amount of water at the interface.

Haefeli's experiments provide partial experimental proof that the relationship between shear stress and glide velocity is linear for rigid body sliding of wet snow over a smooth interface. For the expected field condition of a rougher interface, analysis shows that this constitutive equation would be linear in the general case with a correspondingly higher constant of proportionality. As pointed out previously (McClung, 1975), however, if the water film thickness becomes much greater than the asperity wavelength or if the film thickness between the snow and the asperity becomes greater than a thin film, the drag, τ, will tend to zero as the film thickness increases. An unstable condition will develop, making steady glide impossible. Haefeli's experiments, indeed, show extremely small drag as the meltwater film thickness increases. It is also possible that the linear τ-U_0 relationship will break down as $U_0 \rightarrow 0$; this important aspect of the problem is disregarded in the present formulation.

CONSTITUTIVE RELATIONS FOR THE LUBRICATION SLIDING MECHANISM AND THEIR PHYSICAL BASIS

Let us consider the general case of a snow slab sliding by rigid body motion over a rough interface with the slab separated from the gliding interface by a thin film. Figure 4a depicts the situation.

For the case of slow, steady glide the problem is to solve for the fluid velocity, $\vec{u}$, and the fluctuating water pressure, P, distribution in the film. The relevant equations to be solved, disregarding inertial effects, are

$$\mu_w \nabla^2 \vec{u} - \nabla P = 0$$
$$\nabla \cdot \vec{u} = 0 \tag{30}$$

where μ_w is the viscosity of water at 0°C. In this case, the boundary conditions are in terms of $\vec{u}$ alone, namely $\vec{u} = 0$ on the bed and $\vec{u} = U_0 \hat{e}_x$ on the gliding snow slab. The equations above then reduce to:

$$\nabla^2 (\nabla \times \vec{u}) = 0 \quad , \quad \nabla \cdot \vec{u} = 0 \tag{31}$$

The solution to this problem is of the form (Batchelor, 1967):

$$\vec{u} = U_0 \cdot \left[\text{function } \left(\frac{\vec{x}}{L}, \text{ geometry of boundary conditions} \right) \right] \tag{32}$$

$$P - P_0 = \frac{\mu_w U_0}{L} \cdot \left[\text{function } \left(\frac{\vec{x}}{L}, \text{ geometry of boundary conditions} \right) \right] \tag{33}$$

The shear stress is given by:

$$\tau_{xz} = \mu_w \left(\frac{\partial u}{\partial z} + \frac{\partial w}{\partial x} \right)$$

The shear stress is, in general, of the form

$$\tau = \langle \tau_{xz} \rangle = \frac{\mu_w U_0}{L} \cdot f(\text{geometry of boundary conditions}) \tag{34}$$

where L is indicative of the film thickness. However, it retains this definition only when the faces separated by the fluid are smooth with parallel sides. Several specific solutions are available from lubrication theory, and it is instructive to look at these solutions to understand the physics of the mechanism.

Batchelor (1967) gives the solution for the sliding block tilted at a small angle α sliding over a smooth surface (Fig. 4b). For the geometry of Figure 4b, the τ-U_0 constitutive equation is:

$$\tau = \frac{\mu_w}{\alpha \ell}\left[3\left(\frac{d_1-d_2}{d_1+d_2}\right) - 2 \log \frac{d_1}{d_2}\right] U_0 \tag{35}$$

The pressure is given by:

$$P - P_0 = \frac{6\mu_w}{\alpha}\left[\frac{(d_1-d)(d-d_2)}{d^2(d_1+d_2)}\right] U_0 \tag{36}$$

where $\alpha = \frac{d_1}{\ell} = r$ for the geometry in Figure 4b.

The pressure is supportive only when fluid is forced from the wide to the narrow end of the block. This case is of interest because it is the limiting case of the sinusoidal roughness for low roughness. We could define an equivalent coefficient of friction by τ/σ and this is proportional to $r \simeq \alpha$.

Thus, for a periodic distribution of roughness, we expect a drag to be exerted on the gliding snowpack for a thin enough fluid (water) layer, and it is the geometry, fluid thickness and fluid pressure which control the sliding conditions. If the block or glide interface has a rougher surface, obviously the pressure distribution will be altered and the drag will be changed. Michell (1950) discussed in detail the important case of sinusoidal asperities sliding over a smooth plate. The main result of this significant calculation is that the value of the coefficient of friction decreases as the film thickness approaches the height of the asperities. Greater film thicknesses would result in rapidly diminishing friction.

GENERAL THEORY FOR GLIDE

Obviously, a general theory of snow gliding would be very difficult to formulate and in view of the unknowns involved it would not only be complex but impossible at this time. Since the creep constitutive equation of snow is most likely non-linear and compressible, a general treatment of the creep mechanism would clearly result in a non-linear relationship between τ and U_0, and so in general the glide constitutive equations would be non-linear where there were competing mechanisms. In addition, without further experimental evidence and theory it is impossible to evaluate the mechanism of regelation in spite of the suspicion that its role is negligible or at any rate small.

To point the way toward a general theory, we bypass these shortcomings of our knowledge for the moment and consider a three-mechanism theory based on linear incompressible Newtonian modeling of the constitutive equation describing the internal deformation in the snow slab. We presume that glide is possible by regelation in the manner described above.

When there is no separation, the glide constitutive equation is of the form:

$$\tau = \frac{\mu U_0}{D} = \frac{\mu U_0}{(D_C + D_R)} \tag{37}$$

where D is dependent on the geometry of the glide interface and the physical constants from the regelation physics and snow viscosity. If D is significantly less than the snowpack depth, glide is mostly by creep, and if D is significantly larger than the snowpack depth, glide is mostly by pressure melting. The D depends only on the geometry of the boundary conditions, regelation physics constants, and the snow viscosity. If the film thickness is large enough to drown some of the smaller asperities or if some of the asperities are of low enough roughness, technically there will be separation, and the lubrication sliding mechanism will come into play at various localities, resulting in an increase in glide velocity and an effective increase in the stagnation depth. Gliding experiments in Norway (McClung, 1976b) and in Switzerland on rock slopes that are smooth except for small asperities give some support to this logic. These experiments show very little or no glide until significant amounts of water have reached the interface. This could be interpreted to mean that components of the roughness spectrum were present for small wavelengths, making the creep mechanism very slow with the regelation mechanism not participating. Addition of water at the interface could drown these small wavelength asperities, increasing glide by permitting creep over the longer wavelength asperities and/or local separation at the small wavelength asperities.

If one decomposes the bed into harmonics and makes use of Nye's superposition rule and then if one presumes that regelation in a snowpack is similar to regelation for ice sliding problems, it is the asperity wavelength which controls the competition between these two mechanisms. Short wavelength asperities in this case would be suitable for fast regelation because of a short heat conduction path, whereas creep would be faster over long wavelength asperities. When water began to appear in any quantity, the heat conduction path would be lengthened and regelation would be suppressed. On the other hand, creep might be enhanced and local separation might begin to appear at points of low A/λ.

Therefore, one can say that it is the wavelength which controls the participation of the creep and regelation mechanisms and it is the roughness parameter which determines whether the lubrication sliding mechanism will be competitive. The general form of the glide constitutive equation for the lubrication mechanism is of the form:

$$\tau = \frac{\mu_w}{L} \cdot f(\text{boundary conditions})\ U_0 \tag{38}$$

where L depends only on the geometry.

We can express this in the form of the glide constitutive equation for the other two mechanisms as:

$$\tau = \frac{\mu U_0}{D} \tag{39}$$

where D is now a complicated function of μ, μ_w, geometry and water content. Therefore, the general case of any of the three mechanisms can be expressed in the form of Equation 39 where D is a field measurable parameter.

For the case in which separation does not occur, if D is less than the snowpack depth, glide is mostly by creep, and if D is greater than the snowpack depth, glide is mostly by regelation. When separation occurs, for small r and high slope angles, regelation would be suppressed (if it exists); if D is much less than the snowpack depth, glide is mostly by creep, and if D is greater than the snowpack depth, glide is mostly by lubrication sliding.

For the case of steady glide over a surface other than a rough surface, such as glide over ice layers within the snowpack, we expect the mechanism to be lubrication sliding. There are, however, no steady glide measurements for such surfaces because of the experimental difficulty in locating such a layer and because such situations are

usually expected to be present prior to release of wet slab avalanches when the glide is presumably not steady. This situation is discussed in subsequent sections.

In most cases competition will be possible among these three proposed mechanisms. Field data show a fluctuating component superimposed on the expected behaviour for a creep mechanism. McClung (1975), however, provided data for a case on a timbered slope when the lubrication sliding mechanism was likely somewhat suppressed (Fig. 5). This experiment showed largely steady glide during the middle of the winter and a dependence on snow depth for two different seasons.

POROUS MEDIA EFFECTS FOR STEADY GLIDE

In the case of steady glide by the creep mechanism, it is possible that if the snow in the bottom layers of the snowpack is saturated with water, excess pore pressures may develop and affect the glide boundary conditions. On the other hand, any excess water, such as would exist for saturated snow at the interface, would tend to suppress regelation by lengthening the heat conduction path.

As snow creeps over asperities, there will be zones of high pressure on the upstream sides and zones of low pressure on the downstream sides. This can cause local squeezing out of water on the upstream sides (consolidation) and dilation of the snow on the downstream sides of asperities. If glide was fast enough by the creep mechanism, excess pore pressures could possibly be built up by this mechanism, thereby affecting the glide constitutive equation by the effect of pore pressures on the normal stresses on the asperities. The condition would be that glide would occur faster than excess pore pressures could diffuse away. A simple dimensional analysis of the problem is possible by comparing the half-wavelength of the asperities, $\frac{\lambda}{2}$, with the characteristic diffusion length of c/U_0, where c is the diffusivity. The non-dimensional quantity of relevance is: $\frac{U_0}{c} \cdot \frac{\lambda}{2}$. If this quantity is on the order of or greater than 1, then the above-mentioned porous media effect will be important in the glide problem, i.e., we require:

$$\frac{U_0}{c} \cdot \frac{\lambda}{2} = O(1)$$

For the glide problem, U_0 is on the order of 1-10 mm/day, while λ is expected to range from a fraction of a millimetre to on the order of 0.5 m. At present it is not possible to give accurate values of c. Order of magnitude estimates, however, seem possible based on reasonable values for other materials. For example, for clay c is on the order of 10^{-6} m^2/s, while for porous sandstone c is on the order of 1 m^2/s (Rice and Simons, 1975). For snow, which is very porous and which has a permeability of $\sim 10^4$ that

of clay, we naturally expect values of c much higher than for clay. It is obvious from the expression above, that only for values of c as low as that for clay will the condition above be satisfied. Therefore, we conclude that it is very unlikely that porous media effects will influence steady glide. The basic reason is that steady glide is slow enough to permit dissipation of pore pressures by diffusion through the snow, which is very permeable.

Porous media effects of the above-mentioned kind would not be expected to have any influence on the lubrication sliding mechanism because of the separation of the snowpack, which is necessary for the mechanism to operate. Water pressure of another kind, namely that of free standing water, P_w, having access to the interface may also affect the gliding conditions. In that case the condition for separation may be affected. Following Kamb (1970), we express the water pressure as a fraction, k, of the applied normal stress, σ. The separation condition then becomes for the case of a single wavelength:

$$\frac{\langle 2P^2 \rangle^{\frac{1}{2}}}{\sigma - P_w} = \frac{2}{\pi\sqrt{2}} \frac{\tan \Psi}{(1-k)} \frac{1}{r} \rightarrow 1 \qquad (40)$$

Experience, however, shows that free standing water to any significant depth is rare in the alpine snowpack because either it drains away or is coincident with avalanching, which is not associated with steady glide. However, since the density of alpine snow is usually one-third to one-half that of water, the effect may be felt for thin snowpacks.

GLIDE CONDITIONS FOR NON-NEUTRAL ZONE CASES

The above sections all deal with glide conditions in the neutral zone. However, there are many situations in which a gradient in glide conditions occurs in compressive and tensile zones in the snow cover. Discussion here is limited to the two-dimensional plane strain-rate case.

When there are differences in roughness and water depth along a glide interface, the constitutive relation between shear stress, τ, and glide velocity, U_0, will be a variable relationship rather than a constant. Figure 6 shows the relationships for three possible configurations.

These relationships are analogs of constitutive relations describing plastic failures in thin samples of materials deformed in shear. Figures 6a and 6b depict analogs

of strain-softening behaviours, while 6c is the somewhat more ideal case of the analog of perfect plastic behaviour.

These conditions could result from geometrical conditions at the interface in transition from a region of high roughness to one of low roughness; from varying water content at the glide interface, for example, by inhomogeneous melt or rainwater percolation; or from combinations of these as well as other factors.

For the case in which glide begins at an interface, from a no-glide condition, it is possible that the situation may appear as in Figure 6a. This situation might result if there was bonding between the snowpack and the glide interface. For example, it might occur when meltwater or rainwater reached an interface which was previously dry; melting of bonds takes place analogous to a failure of dry snow. Slow shear failures of dry snow samples often show stress-displacement curves like that of Figure 6a (McClung, 1977), i.e., strain-softening type failures. Shear experiments on dry snow show that strain-softening experiments are accompanied by dilation owing to interparticle interference and other factors. It may well be that when melt takes place and destroys bonds in a given region, for example, coincident with the start of sliding over an ice interface, there may be less interference to sliding and dilation need not be present. Shear stress-glide velocity distributions, as in Figures 6a and 6b, are viscous analogs of strain-softening curves of shear stress-displacement observed for failures of dry snow and other geotechnical materials.

Non-neutral zone conditions imply size effects in the snow gliding problem. One unknown size is the implied distance along the glide interface in which the shear stress falls from its maximum to its minimum value. At present it is not possible to estimate those kinds of size effects because relevant experimental data relating shear drag to glide velocity do not exist. It seems logical, however, that a wide range of these size effects may exist. For example, the water content at the glide interface might increase for long distances downslope, which would produce a continual reduction in shear stress with downslope distance. Such size effects are well recognized for strain-softening failures in geotechnical materials, such as clays prior to the onset of shear band propagation (Palmer and Rice, 1973; Cleary and Rice, 1974), as well as for failures in dry snow (McClung, 1979).

Wet Slab Avalanche Release

When the conditions at the glide interface are such that the glide velocity increases in the downslope direction, the process is analogous to plastic yielding in an infinitely thin zone. Probably the most important glide mechanism is lubrication-sliding for wet slab avalanche release because such a mechanism is concurrent with low values of friction and high gliding velocities at the sliding interface. In such a case the proper boundary condition is a relationship between shear stress and glide velocity which must be provided by experimental measurements. The transition region from a region of slow glide to a region of fast glide is, then, characterized by a process analogous to strain-softening, which is observed in shearing of many materials including dry snow. This transition region is called the breakdown zone. We do not, however, expect that the fracture mechanical ideas that were applied to the dry slab in McClung (1979) will be strictly applicable to the wet slab problem, the reason being that when separation occurs, a water film separates the slab from the substratum and a fracture mechanical stress-*displacement* relationship would be inappropriate.

We intuitively expect that the relationship between shear stress and glide velocity will involve a drop in shear stress accompanied by a rise in glide velocity downslope from a region of relatively slower gliding. This process will involve an important size effect in the breakdown zone, which is the distance along the glide surface in which the shear stress drops from its peak to its lowest (residual) value. This latter value could be near zero in the case of unstable separation. It is clear that this size effect will be heavily dependent on the substratum geometry and water content along the glide surface and that we have no known way to evaluate it in general. We do, however, anticipate that the breakdown physics will be an important aspect of wet slab avalanche release.

Another important aspect of the problem, as we shall see, involves the rise of shear stress beyond the breakdown zone once a residual value is reached. This also will involve a size effect for recovery to a neutral zone value of shear stress and glide velocity appropriate to the interface conditions in the recovery zone. The size effect will also depend upon the water content and substratum geometry. This zone is called the recovery zone. If we assume no gradients in water content and substratum geometry in the recovery zone, this part of the problem is amenable to solution because relationships between shear stress and glide velocity for steady glide can be used. Figure 7 shows a possible relationship between shear stress and glide velocity downslope.

Our interest focuses on the tensile stress conditions in the body of the slab for typical slab parameters. Since the character of the breakdown zone is unknown, a case must be developed where the breakdown zone can be compared with the slab height H and then we can easily analyze the case for small breakdown zones from this more general result. The modeling below is intended to be for full depth wet avalanche release where there is roughness at the glide interface. Obviously, for wet slabs sliding over a smooth ice interface in the pack the modeling may be analogous but the friction drop might occur very rapidly so that the quasi-static approach breaks down.

SLAB STRESS CONDITIONS FROM A ONE-DIMENSIONAL MODEL

To study tensile stresses in the snow slab under a changing shear stress boundary condition, we specialize to a one-dimensional model and we assume in this approximation that most of the deformation is on the glide surface rather than in the slab. We further assume that the substratum is much harder than the slab material, as this is the case for most wet slab avalanches where typical substrata are ice layers or the ground, so that the surface is impermeable to water. In our model, we shall average quantities over the depth of the slab (or snowpack):

$$\bar{\sigma} = \frac{1}{H} \int_0^H \sigma_{xx} dz$$

To analyze the simplest case we develop the model for the situation in Figure 7. Since the boundary condition in the breakdown zone is unknown, we assume that the drop in shear stress is linear with distance in the transition from a wet interface to a much wetter interface. Once the interface is fully wetted, we assume for simplicity constant water content and geometry at the interface and this, as we shall see, implies a size for the recovery zone.

For the one-dimensional scheme described above, we can write the equilibrium condition by averaging over z dependence as:

$$H \frac{d\bar{\sigma}}{dx} = \bar{\rho} g H \sin \Psi - \tau(x) = \tau_g - \tau(x) \qquad (41)$$

where $\tau(x)$ denotes the distribution of shear stress as a function of x.

We further assume that the slab material is linear viscous, characterized by a constitutive equation:

$$\bar{\sigma} = E'\bar{\dot{e}} - \bar{P}_0 \tag{42}$$

and where the extensional strain-rate is:

$$\bar{\dot{e}} \simeq - \frac{du}{dx} \tag{43}$$

For a homogeneous slab, $\bar{P}_0$ is given by:

$$\bar{P}_0 = \frac{1}{2} \left(\frac{\nu}{1-\nu} \right) \bar{\rho} g \cos \Psi H$$

From Figure 7, the following boundary conditions can be written:

$\tau \to \tau_g$ for $x = 0$ and $x \to \infty$

$u = U_0$ for $x \to \infty$

$\bar{\dot{e}} = 0$ for $x \to \infty$

$\bar{\dot{e}} = \bar{\dot{e}}_0$ for $x = x_0$

$u = U_R$ for $x = x_0$

$\tau = \tau_R$ for $x = x_0$

$u = 0$ for $x = 0$

For the recovery zone we wish to satisfy a glide constitutive equation of the form:

$$\tau = \frac{\mu}{D} u = ku \tag{44}$$

in accord with our treatment of snow gliding theory.

First we consider the recovery zone:

$\infty > x \geq x_0$

We multiply Equation 41 by $\bar{\dot{e}}$ and integrate to get:

$$\int_{x_0}^{x} H\bar{\dot{e}} \frac{d\bar{\sigma}}{dx} dx = \int_{x_0}^{x} [\tau_g - \tau(x)] - \left(\frac{du}{dx}\right) dx \tag{45}$$

Using Equations 44 and 42 in Equation 45 gives the condition

$$\frac{HE'}{2} (\bar{\dot{e}}_0^2 - \bar{\dot{e}}^2) = \tau_g u - \frac{1}{2} ku^2 \tag{46}$$

or

$$\bar{\dot{e}}^2 = \left(\frac{du}{dx}\right)^2 = \bar{\dot{e}}_0^2 - \left(\frac{2\tau_g u}{HE'} - \frac{ku^2}{HE'}\right) \tag{47}$$

This is a non-linear differential equation. Since $u = U_0$ and $\bar{\dot{e}} = 0$ for $x \to \infty$, we get:

$$\bar{\dot{e}}_0 = \left(\frac{\tau_g U_0}{HE'}\right)^{\frac{1}{2}} = \left(\frac{\tau_g^2}{kHE'}\right)^{\frac{1}{2}} \tag{48}$$

Substituting this into Equation 47 then yields:

$$\frac{du}{dx} = \pm \sqrt{\frac{k}{HE'}} \left(\frac{\tau_g}{k} - u\right) \tag{49}$$

If we reject the (+) solution so that the result is well behaved for large x, solution of Equation 49 for the boundary conditions above yields:

$$u = \frac{\tau_g}{k} - \frac{\tau_g}{k} \left(1 - \frac{\tau_R}{\tau_g}\right) \exp - \sqrt{\frac{k}{HE'}} (x - x_0) \tag{50}$$

for $\infty > x \geq x_0$.

For the region $x_0 \geq x \geq 0$, we take a linear distribution of shear stress, for example:

$$\tau(x) = \tau_g - \frac{x}{x_0} (\tau_g - \tau_R) \tag{51}$$

Substituting this into Equation 41 yields:

$$\int_{\bar{\sigma}(x_0)}^{\bar{\sigma}(x)} d\bar{\sigma} = - \int_{x_0}^{x} \frac{x}{x_0 H} (\tau_g - \tau_R) \, dx \tag{52}$$

Integrating gives for $x_0 \geq x \geq 0$,

$$\bar{\sigma}(x) = \bar{\sigma}(x_0) + \frac{x_0}{2H} (\tau_g - \tau_R) - \frac{x^2}{2x_0 H} (\tau_g - \tau_R) \tag{53}$$

From Equation 50, we can calculate $\sigma(x)$ for $\infty > x \geq x_0$ in conjunction with Equation 42:

$$\bar{\sigma}(x) = \tau_g \sqrt{\frac{E'}{kH}} \left(1 - \frac{\tau_R}{\tau_g}\right) \exp - \sqrt{\frac{k}{HE'}} (x - x_0) - \bar{P}_0 \tag{54}$$

For $\bar{\sigma}(x_0)$, we get from this:

$$\bar{\sigma}(x_0) = \tau_g \sqrt{\frac{E'}{kH}} \left(1 - \frac{\tau_R}{\tau_g}\right) - \bar{P}_0 \tag{55}$$

The maximum tensile stress will be found at $x = 0$ as:

$$\bar{\sigma}(0) = \tau_g \sqrt{\frac{E'}{kH}} \left(1 - \frac{\tau_R}{\tau_g}\right) + \frac{x_0}{2H} (\tau_g - \tau_R) - \bar{P}_0 \tag{56}$$

where we have not yet defined x_0.

Use of Equation 53 in conjunction with the constitutive equation yields:

$$\frac{du}{dx} = \frac{\tau_g}{\sqrt{E'kH}} \left(1 - \frac{\tau_R}{\tau_g}\right) + \frac{\tau_g - \tau_R}{2HE'} \left(x_0 - \frac{x^2}{x_0}\right) \tag{57}$$

Integrating this and using the condition u = 0 when x = 0 gives:

$$u = \frac{\tau_g}{\sqrt{E'kH}} \left(1 - \frac{\tau_R}{\tau_g}\right) x + \frac{\tau_g - \tau_R}{2HE'} \left(x_0 x - \frac{x^3}{3x_0}\right) \tag{58}$$

The condition $u = U_R$ when $x = x_0$ gives:

$$\left(\frac{\tau_g - \tau_R}{3HE'}\right) x_0^2 + \frac{\tau_g}{\sqrt{E'kH}} \left(1 - \frac{\tau_R}{\tau_g}\right) x_0 - U_R = 0 \tag{59}$$

This is a quadratic equation with a positive root given by:

$$x_0 = \sqrt{\frac{2HD}{1-\nu}} \left(\sqrt{\frac{9}{4} + \frac{3}{(\tau_g/\tau_R - 1)}} - \frac{3}{2}\right) \tag{60}$$

to provide an estimate of the breakdown zone length where we have used Equation 44 and where $E' = \frac{2\mu}{1-\nu}$ in terms of the shear viscosity, μ, and the viscous analog of Poisson's ratio.

Similarly, we can express $\bar{\sigma}(0)$ as:

$$\bar{\sigma}_{max} = \bar{\sigma}_0 = \tau_g \sqrt{\frac{2}{1-\nu} \frac{D}{H}} \left(1 - \frac{\tau_R}{\tau_g}\right) + \frac{x_0 \tau_g}{2H} \left(1 - \frac{\tau_R}{\tau_g}\right) - \bar{P}_0 \tag{61}$$

for the maximum value of tensile stress. For the case of small breakdown zone, x_0, this reduces to:

$$\bar{\sigma}_{max} \simeq \tau_g \sqrt{\frac{2}{1-\nu}\frac{D}{H}} \left(1 - \frac{\tau_R}{\tau_g}\right) - \bar{P}_0 \tag{62}$$

For Equations 60 and 61 our interest focuses on the conditions when the tensile strength of the slab material is approached in the slab by the maximum principal stress and when the angle between the maximum principal stess and the glide interface, γ, is 10° or less (Perla and LaChapelle, 1970).

Accordingly, the definition of γ is:

$$\gamma = \frac{1}{2} \tan^{-1} \left(\frac{2\tau_{xz}}{\sigma_{xx} - \sigma_{zz}}\right) \tag{63}$$

For the one-dimensional approximation this can be expressed roughly as (at the glide interface):

$$\gamma \simeq \frac{1}{2} \tan^{-1} \left(\frac{1}{\frac{\bar{\sigma}_{max}}{2\tau_g} + \frac{\cot \Psi}{2}}\right) \tag{64}$$

at x = 0. Similarly, the maximum principal stress is:

$$\sigma_1 = \frac{\sigma_{xx} + \sigma_{zz}}{2} + \left[\left(\frac{\sigma_{xx} - \sigma_{zz}}{2}\right)^2 + \tau_{xz}^2\right]^{\frac{1}{2}} \tag{65}$$

which can be expressed as (at the glide interface):

$$\frac{\bar{\sigma}_1}{\tau_g} \simeq \left(\frac{\bar{\sigma}_{max}}{2\tau_g} - \frac{\cot \Psi}{2}\right) + \left[\left(\frac{\bar{\sigma}_{max}}{\tau_g} + \cot \Psi\right)^2 \frac{1}{4} + 1\right]^{\frac{1}{2}} \tag{66}$$

at x = 0.

Figure 8 depicts $\bar{\sigma}_1/\tau_g$ and Figure 9 gives γ as functions of D/H and ν for $\tau_g/\tau_R = 2$ and $\tau_g/\tau_R = 10$ with $\Psi = 45°$. Figure 10 gives predictions of the breakdown zone length as functions of Poisson's ratio and relative stagnation depth.

We can also estimate the recovery zone length by observing that the glide velocity returns to 99% of the neutral zone value in the distance

$$x' \simeq 5\sqrt{\frac{HE'}{k}} = 5\sqrt{\frac{2HD}{1-\nu}} \tag{67}$$

from Equation 50. For example, if $\nu = 0.2$ and D/H ranges from $\frac{D}{H} = \frac{1}{2}$ to $\frac{D}{H} = 3$, x' is approximately between 5.6 H and 13.7 H. The length underneath the slab under which the glide conditions are perturbed from their neutral zone values is approximately $x_0 + x' \simeq 6H$ to 16 H according to the one-dimensional model presented here.

For the model presented here, rather vigorous gliding (large D) is needed to bring the maximum principal stress near to 10° of the perpendicular to the glide interface, and low residual friction is also required. It should be remembered that the model is one-dimensional and assumes that most of the deformation occurs at the glide layer. Finite element calculations may predict quite different results when deformation in the slab is accounted for.

The results presented here indicate that separation and lubrication sliding are the important glide considerations for wet slab avalanche release, and presumably, very smooth surfaces and a large quantity of water must be present over a significant basal region on a steep slope to precipitate release.

The two key parameters in the present theory are the relative stagnation depth, D/H, and viscous analog of Poisson's ratio. Since the equations do not vary greatly with Poisson's ratio, it is likely that the boundary condition at the glide interface controls the release.

The model chosen is, of course, very idealized, but it indicates features that should be present with respect to release of wet slab avalanches. The breakdown zone can be large with respect to slab thickness H and is analogous to a strain-softening failure in solid materials. The recovery zone in which we have taken constant water content and geometry may not display these conditions, and therefore it could be much larger than our predictions if a gradient in water content prevented shear stress recovery. It would be relatively easy to generate a region in which boundary conditions are perturbed over 25 H in this way. In this sense, our model

stands as a prediction for minimum tensile stresses in the slab and maximum angles, γ.

This treatment of the wet slab avalanches has to be regarded as an approximation. In reality, there will be a distribution of pressure in the water film at the base of the slab which can make water flow perturb the boundary conditions from the simple model given here.

It is remarkable, however, that the relative stagnation depth D/H = 3 necessary to rotate the maximum principal stress to within 15° of the glide plane is in accord with the fastest gliding measurements in Switzerland. For such conditions, glide crack formation roughly perpendicular to the slope would be imminent according to the present model. For D/H much less than this value slab tensile stresses presumably are not high enough to crack the slab. It should also be remarked that once a tensile crack begins to form near the glide interface, the fracture angle, γ, will decrease toward 0° as the length of the tensile crack increases.

THE FRACTURE MECHANICAL ASPECT OF WET SLAB AVALANCHE RELEASE

A process of the type described above might also result in a progressive type of failure. In other words, the breakdown zone might tend to be driven upslope by itself. This kind of failure has analogies to a crack-like shear fault propagation as we shall see below. To describe the propagation of the breakdown zone we consider first an energy balance approach to the problem. Such an approach lends itself well to the case considered here in which the slab is considered to deform inelastically (viscously).

Considering an uphill displacement of the breakdown zone by a distance dL, we specialize to the case in which the breakdown zone is small. The strain-rate and stress at the breakdown zone after it has been displaced by dL are $\bar{\dot{e}}(x_0)$ and $\bar{\sigma}'(x_0)$. Then the net downslope work/unit time to displace the material outside the breakdown zone by dL is:

$$H\bar{\dot{e}}(x_0)\bar{\sigma}'(x_0)dL$$

This should balance the stress work in deforming the material in the slab plus the frictional dissipation on the sliding surface in the end zone. Figure 11 depicts the situation and the resulting equation is:

$$H\bar{\dot{e}}(x_0)\bar{\sigma}'(x_0)dL = HdL\int_0^{\bar{\dot{e}}(x_0)} \bar{\sigma}d\bar{\dot{\varepsilon}} + dL\int_0^{U_R} \tau(u)du \tag{68}$$

Dividing this equation by dL and integrating by parts gives:

$$H\int_{-P_0}^{\bar{\sigma}'(x_0)-\bar{P}_0} \bar{\dot{e}}(\bar{\sigma})d\bar{\sigma} = \int_0^{U_R} \tau(u)du \tag{69}$$

If we now use the linear constitutive equation and with

$$\bar{\sigma}'(x_0) = \sqrt{\frac{2}{1-\nu}\frac{D}{H}}\ \tau_g\left(1 - \frac{\tau_R}{\tau_g}\right)$$

as before, we get the propagation condition:

$$\frac{H}{2E'}\left[\frac{2}{1-\nu}\frac{D}{H}(\tau_g - \tau_R)^2\right] = \int_0^{U_R} \tau(u)du \tag{70}$$

The term on the left represents the driving force term and that on the right represents the resistance to expansion of the breakdown zone upslope. When this equation is satisfied we can expect quasi-static advance of the breakdown zone upslope. If we use, for example, a breakdown zone stress-velocity distribution and average it over the breakdown zone, Equation 70 can be rewritten:

$$\frac{D}{2\mu}(\tau_g - \tau_R)^2 = (\tau_p - \tau_R)\ \langle u\rangle \tag{71}$$

This result could have been written immediately from the small-scale yielding result from crack mechanics in terms of a stress concentration factor for a semi-infinite crack within an infinite strip of height 2 H:

$$K \simeq \sigma' (x_0) \sqrt{\frac{H}{2}} \tag{72}$$

The propagation condition is given by Palmer and Rice (1973):

$$\frac{1-\nu}{2\mu} K^2 = \int_0^{U_R} \tau(u)\, du \tag{73}$$

which is for the case in which the breakdown zone is small with respect to slab H and length. The slip velocity (displacement/unit time) at the end of the breakdown zone is represented by U_R. When Equation 72 is satisfied, we expect a quasi-static motion uphill of the breakdown zone. This will permit the failure surface to expand outwards. The same kind of argument could, of course, be given for the case of anti-plane shearing in which Equation 73 would be replaced by:

$$\frac{1}{2\mu} K'^2 = \int_0^{U_R} \tau(u)\, du \tag{74}$$

if the failure surface was loaded laterally as well as upslope. Conditions 73 and 74 will be recognized from the work of Palmer and Rice (1973) as equivalent to the small-scale yielding condition of fracture mechanics. An important difference exists, however, as we are dealing mainly with inelastic deformation in the slab. Therefore, Equation 70 is only approximately valid because in its derivation the stress-work in the breakdown zone deformations is assumed to be fully recovered.

Another important difference here is that the "yield stress" analog, τ_p, can be near to τ_g and it is still possible to be able to use the small breakdown zone approximation. This would not be possible if we dealt with a problem of yielding of a material. In fact, we think that in many cases for the wet slab problem $\tau_p \simeq \tau_g$. Certainly, one would expect that $\tau_p > \tau_g$ if glide actually begins from a totally dry interface condition upslope.

From these considerations it seems possible for the failure surface to expand progressively to undercut a slab. For the simplified case given here for constant water content in the recovery zone this would eventually result in a "mature" shear band analog in which the tensile stresses would not increase to more than

$$\bar{\sigma} \simeq \sqrt{\frac{2}{1-\nu}\frac{D}{H}}\ \tau_g \left(1 - \frac{\tau_R}{\tau_g}\right) - \bar{P}_0$$

for the small breakdown zone.

However, tensile stresses of this order are enough to produce a tensile crack in the slab which can result in avalanche release by subsequent loading of the glide surface. The situation could be radically different from the simple picture presented here for an actual field situation. If the water content increased continually downslope in the recovery zone, for example, much higher tensile stresses would be possible and, in addition, a finite-sized breakdown zone would have the same effect of increasing tensile stresses. Furthermore, the expansion of the failure surface would no longer be quasi-static.

It should also be pointed out that once a tensile crack appears, the calculations above are no longer valid.

TIMING OF WET SLAB AVALANCHE RELEASE AND POROUS MEDIA EFFECTS

The timing aspects of wet slab avalanche release are keyed to the distribution of water pressure on the glide interface in the present problem. The water pressure at the glide interface depends on the availability of water and the basal shear stress. The separation process in the breakdown zone could result in a propping up (dilation) of the slab, which can result in suctions which can increase the effective compressive stress at the glide interface and, thereby, possibly stabilize breakdown zone spreading. In addition, however, there will be a pressure gradient along the glide interface (since there is a distribution of shear stress there). For a steep enough stress distribution in the breakdown zone, this effect will tend to force water into the breakdown zone as a counterbalance to the suction effect mentioned above and promote breakdown zone motion and expansion. The interplay between these kinds of effects is likely to be an important aspect of the timing problem. Quantitative evaluation of the timing problem is deferred to a later study.

Of course, if the driving stress is increased over that given by the left side of Equation 71 by a rapid increase of lubrication in the recovery zone or by non-uniform water content in the recovery zone, then the "failure" surface may rapidly expand uphill and laterally, eventually producing tensile cracking through the body of the slab. On the other hand, advance of the breakdown zone may be stopped by some kinds of geometrical considerations, for example, in the case of full depth slabs, if a severe change in the roughness characteristics at the glide interface is encountered.

Curiously, the one-dimensional model is not likely to exhibit stabilizing porous media effects in most cases. For fast enough propagation velocities one might expect the wet slab material to respond in an undrained fashion without the possibility of fluid mass transfer and an upper limit undrained Poisson ratio of $\nu_u \simeq 0.5$. For slow propagation, the Poisson ratio of the slab material would be unaffected by pore pressures. The diffusion length scale in the problem is the ratio of the diffusivity to the glide velocity. For the formalism developed by Rice and Simons (1975), for spreading shear disturbances in *elastic* porous media, the length scale c/U_0 gives the dimension of the region around the tip of the spreading disturbance for which properties may be assumed to take their drained values. As mentioned previously, we do not have good estimates of c, but we expect it to be much greater than the 10^{-6} m^2/s adoptable for clays. It is probably safe to assume that c is at least two orders of magnitude larger for snow than for clay. Indeed, if we use the formalism of Rice and Cleary (1975) for the diffusivity for the *elastic* case, this seems to be correct. For saturated snow, their formalism yields a value of c approximately

$$c = K\left[\frac{2G(1-\nu)}{(1-2\nu)}\right]$$

where K is the permeability, G is the shear modulus, and ν is the drained Poisson ratio. From Dunne *et al.* (1976), values of permeability can be extracted. Taking the lower limit of these values we get $K \simeq 10^{-12}$ m^2. Mellor (1964) gives $\sim 10^8$ N/m^2 for G. Using these values with $\nu = 0.25$, we get a *lower limit* value of c of $\sim 10^{-4}$ m^2/s. If we adopt this value, the diffusion length scale is (with $U_0 \sim 10^{-6}$ m/s) $c/U_0 \sim 100$ m, and therefore, the entire slab may be viewed effectively as drained for glide speeds of ~0.1 m/day according to the logic of Rice and Simons (1975).

For either the low speed or high speed limit the driving stress in the propagation condition (73) is unaffected by porous media effects. From the work of Rice and Simons (1975), however, the possibility of stabilizing porous media effects at intermediate speeds seems possible. From their work, the region at the tip of a propagating shear disturbance is always to be considered drained at finite speeds. At slow speeds, the entire slab may be considered to have drained properties. At very high speeds, the region taken to have drained properties shrinks to zero. At intermediate speeds, it is possible for a drained region to exist at the breakdown zone tip, whereas the rest of the slab is to be considered undrained. In that case, K, in the propagation condition, may be taken to have drained properties, and the Poisson ratio in Equation 73 may be taken as an undrained value. This will result in an increasing reduction in the driving stress for some range of speeds up to a maximum of $\frac{1-\nu_u}{1-\nu}$. This factor is two thirds if $\nu_u = 0.5$ and $\nu = 0.25$. Rice and Simons indicate that this effect will begin

for speeds for which $L/(c/U_0)$ approaches 1 or greater, where L is on the order of the length of the recovery zone. If we take L as 10 m and c as our former estimate of 10^{-4} m^2/s, it is evident that the effect begins to assume importance for speeds greater than 1 m/day. However, there is considerable uncertainty about the magnitude of c. In addition, any saturated zone will probably be quite thin with respect to slab height, so that more detailed modeling is required.

Anti-plane spreading is apparently relatively unaffected by porous media effects for any glide speed. Proper accounting, however, can only be done for three-dimensional modeling.

Interruption of Creep and Glide Processes behind Structures

Design of structures to be placed on snow-covered mountain slopes often requires knowledge of the forces resulting from interruption of creep and glide processes in the snow cover. The most important problem in this regard is the pressure exerted at the centre of a structure which runs across the slope for a long enough distance so that edge effects can be disregarded. In two dimensions this is the classic plane strain problem, which can be solved only by numerical methods.

As we shall see, the manner in which glide is interrupted in the zone of influence of the structure is important in determining the range of boundary conditions at the glide interface.

Haefeli (Bader *et al.*, 1939, 1948) tried to formulate an essentially one-dimensional model for snow pressure. His formulation, while predicting reasonable values of snow pressure in some cases, cannot always be relied upon to give accurate results, and it cannot be derived from modern continuum mechanics, since many of his assumptions are in conflict with continuum mechanics. Nevertheless, many of his physical assumptions are reasonable.

It is the intent of the model here to apply a continuum mechanical approach to the one-dimensional snow pressure problem. Many of the assumptions used are equivalent to Haefeli's assumptions. As we shall see, such a model provides reasonable values for snow pressure as well as indicating a physical origin for the factors in the snow pressure equations, since the present model turns out to be very similar in form to Haefeli's equations. We limit ourselves to linear creep and glide constitutive equations in this study.

DISTRIBUTION OF GLIDE VELOCITY BEHIND A STRUCTURE

Let us consider the geometry of Figure 12 and average quantities through the depth of the snowpack as we have done before. The snowpack is assumed stiff initially so that most of the deformation takes place along the glide interface. Viscous motion is considered in the x direction only.

As before, we define quantities

$$\bar{\sigma} = \frac{1}{H} \int_0^H \sigma_{xx} \, dz$$

The equation of equilibrium is:

$$H \frac{d\bar{\sigma}}{dx} = \bar{\rho} g H \sin \Psi - \tau(x) = \tau_g - \tau(x) \tag{75}$$

For this problem we use a linear viscous constitutive equation:

$$\bar{\sigma} = E' \bar{\dot{e}} - \bar{P}_0 \tag{76}$$

We define the strains as:

$$\bar{\dot{e}} \simeq - \frac{du}{dx}$$

and

$$\bar{P}_0 = \frac{1}{H} \left(\frac{\nu}{1-\nu} \right) \int_0^H z \rho g \cos \Psi \, dz = \frac{\nu}{1-\nu} \bar{\rho} g \cos \Psi \cdot \frac{H}{2}$$

For the geometry of Figure 12, we can write some boundary conditions:

$$\begin{aligned} &u = 0 \quad \text{at} \quad x = 0 \\ &\bar{\dot{e}} = \bar{\dot{e}}_{max} \quad \text{at} \quad x = 0 \\ &u = U_0 \quad \text{for} \quad x \to \infty \\ &\bar{\dot{e}} = 0 \quad \text{for} \quad x \to \infty \end{aligned} \tag{77}$$

where U_0 is the neutral zone value of the glide velocity.

If we multiply Equation 75 by $\bar{\dot{e}}$ and integrate, we get:

$$\int_0^x H \bar{\dot{e}} \frac{d\bar{\sigma}}{dx} \, dx = \int_0^x \left[\tau_g - \tau(x) \right] \left(- \frac{du}{dx} \right) dx \tag{78}$$

Using the linear constitutive law gives:

$$\int_{\bar{\dot{e}}_{max}}^{\bar{\dot{e}}} E'H\bar{\dot{e}}\, d\bar{\dot{e}} = \int_{0}^{u} -\left[\tau_g - \tau(u)\right]\, du \tag{79}$$

Now along the glide interface, we wish to satisfy a glide constitutive equation of the form $\tau = ku$ where $k = \mu/D$ and where D is dependent only on the water content and interface geometry behind the structure, which is assumed constant along the interface.

Integrating Equation 79 gives:

$$\frac{HE'}{2}\left(\bar{\dot{e}}^2_{max} - \bar{\dot{e}}^2\right) = \left[\tau_g u - \frac{1}{2} ku^2\right]$$

or (80)

$$\bar{\dot{e}}^2 = \left(\frac{du}{dx}\right)^2 = \bar{\dot{e}}^2_{max} - \left(\frac{2\tau_g u}{HE'} - \frac{ku^2}{HE'}\right)$$

This is a non-linear differential equation. Since $u = U_0$ and $\bar{\dot{e}} = 0$ for $x \to \infty$, we can express $\bar{\dot{e}}_{max}$ as

$$\bar{\dot{e}}_{max} = \left(\frac{\tau_g U_0}{HE'}\right)^{\frac{1}{2}} = \left(\frac{\tau_g^2}{kHE'}\right)^{\frac{1}{2}} \tag{81}$$

Substituting this relation into Equation 80 then yields:

$$\frac{du}{dx} = \pm\sqrt{\frac{K}{HE'}}\left(\frac{\tau_g}{k} - u\right) \tag{82}$$

We reject the (+) solution so that our solution is well behaved for large x, and with $u = 0$ at $x = 0$, we get:

$$u = \frac{\tau_g}{K}\left(1 - e^{-\sqrt{\frac{k}{HE'}}\, x}\right) \tag{83}$$

Using the constitutive equation, we can calculate the pressure on the structure for this simple model:

$$\bar{\sigma}(0) = -E' \left.\frac{du}{dx}\right|_{x=0} - \bar{P}_0 \tag{84}$$

$$\bar{\sigma}(0) = -\tau_g \sqrt{\frac{2}{1-\nu}\frac{D}{H}} - \frac{\nu}{1-\nu}\bar{\rho} g \cos\Psi \cdot \frac{H}{2} \tag{85}$$

where the second term represents the static pressure and where we have taken constant density. This formulation will underestimate the snow pressure on a structure, since no proper account is taken of the interruption of the creep processes in the snowpack.

A ONE-DIMENSIONAL MODEL OF SNOW PRESSURE

Now we wish to account for the interruption of creep processes in the snowpack by the structure. To do this in an approximate way in the context of our one-dimensional model, we wish to write a constitutive equation of the form:

$$\tau = k'u \tag{86}$$

for the creep and glide processes. This will guarantee that creep velocities are interrupted in the same manner that the glide velocity is interrupted. The constitutive equation appropriate for glide only is:

$$\tau = \frac{\mu}{D} u_g$$

To include creep, we must decrease k. To do this we view the creep and the glide with stiffnesses coupled in series (Fig. 13), one with stiffness $k_1 = \frac{\mu}{D}$ to account for glide and the other with $k_2 = \frac{\mu}{D_2}$ to account for creep. We could view the problem for glide only with $k_1 = \frac{\mu}{D}$ and $k_2 \to \infty$. For two stiffness constants in series an equivalent k' is given by:

$$k' = \frac{k_1 k_2}{k_1 + k_2} \quad \text{or} \quad \frac{1}{k'} = \frac{1}{k_1} + \frac{1}{k_2} \tag{87}$$

The problem then is the missing length scale D_2. Geometrical considerations (Fig. 13) similar to those for D, however, indicate that D_2 is some function of H, i.e., $D_2 = \alpha H$ where $0 \leq \alpha \leq 1$ where obviously $\alpha = 0$ represents the problem for $k_2 \to \infty$. If we think of the snowpack as deforming in simple shear (Fig. 13), we can write a simple relationship by the definition of strain as (Fig. 13):

$$\tau = \frac{\mu U_A}{H}$$

where U_A is the creep velocity at the top of the snowpack. If we assume a triangular velocity profile, then in terms of the average creep velocity in the layer we can write:

$$\tau = \frac{\mu u_c}{\frac{1}{2} H} = k_2 u_c$$

Combining this in the manner described above with the glide constitutive equation gives:

$$u = u_g + u_c = \tau \left(\frac{1}{k_1} + \frac{1}{k_2} \right)$$

Now combining k_2 with the glide stiffness as in Equation 87, we get:

$$k' = \frac{\mu}{D + \frac{1}{2} H} \tag{88}$$

If we now repeat the derivation for Equations 83 and 85, assuming k' replaces k, we get:

$$u = \frac{\tau_g}{k'} \left(1 - e^{-\sqrt{\frac{k'}{HE'}} x} \right) \tag{89}$$

and

$$\bar{\sigma}(0) = - \bar{\rho} g H \sin \Psi \left[\sqrt{\left(\frac{2}{1-\nu} \right) \left(\frac{D}{H} + \frac{1}{2} \right)} \right] - \frac{\nu}{1-\nu} \bar{\rho} g \frac{H}{2} \cos \Psi \tag{90}$$

The second term represents the static pressure term, and the first term represents the average "dynamic" pressure. The average pressure on the structure is represented by $\bar{\sigma}(0)$.

To calculate the actual snow pressure for engineering applications, the most negative principal stress must be known. For the one-dimensional model, since the shear stress is zero at the structure, it is clear that the most negative principal stress, $\bar{\sigma}_1$, is given as:

$$\bar{\sigma}_1 = -\left[\sqrt{\left(\frac{2}{1-\nu}\right)\left(\frac{D}{H}+\frac{1}{2}\right)} + \frac{\nu}{1-\nu}\frac{\cot\Psi}{2}\right]\bar{\rho}gH\sin\Psi \tag{91}$$

which is the same as $\bar{\sigma}(0)$.

It is instructive to compare the model with the equations of Haefeli (1948) and with the results of finite element calculations. Haefeli's expression for the pressure can be expressed as (Salm, 1977):

$$\bar{\sigma}_H(0) = -\frac{\bar{\rho}Hg}{2\cos^2\Psi}\left[\left(1 - 2\tan\beta_{45^\circ}\right)\cos^3\Psi + \frac{1}{3}\left(\frac{2}{\tan\beta_{45^\circ}}\right)^{\frac{1}{2}}\sin 2\Psi\left(1+\frac{3D}{H}\right)^{\frac{1}{2}}\right] \tag{92}$$

By definition of the creep angle, $\tan\beta_{45^\circ} = \frac{1}{2}\left(\frac{1-2\nu}{1-\nu}\right)$ and this expression becomes:

$$\bar{\sigma}_H(0) = -\bar{\rho}gH\sin\Psi\left[\frac{2}{3}\left(\frac{1-\nu}{1-2\nu}\right)^{\frac{1}{2}}\frac{1}{\cos\Psi}\left(1+\frac{3D}{H}\right)^{\frac{1}{2}}\right] - \frac{\nu}{1-\nu}\bar{\rho}g\frac{H}{2}\cos\Psi \tag{93}$$

Since the expressions for the static pressure are equivalent for these models, we wish to compare the quantities in the brackets for Equations 90 and 93, which we shall denote as C. We compare the two models with finite element calculations by the method outlined by McClung (1976a), assuming a linear viscous creep constitutive equation to describe the deformation of the snowpack and a linear glide constitutive equation at the glide interface represented by line spring elements. Figure 14 shows the comparison of the models with finite element calculations for D/H = 0.2 as a function of viscous

Poisson's ratio. Figure 15 shows the comparison as a function of D/H for $\nu = 0.25$. Both of these comparisons are for $\Psi = 45°$. Figure 16 shows a typical comparison of pressure as a function of depth from the two-dimensional finite element calculations and the two models.

For Figures 14 to 16 illustrate some points worth mentioning. They show that the present one-dimensional model displays the correct dependence on D/H and ν in the range of interest when compared with the numerical equations. Haefeli's equations, on the other hand, display quite a different dependence on these parameters.

For Figures 14 and 15, the value of C plotted for the finite element calculations is the most negative principal stress near the centre of the structure. For Figure 16, for example, the value taken is C = 1.72. It is evident from Figures 14 to 16 that the one-dimensional model provides an average representative pressure on the structure. This is also the intent of Haefeli's model, as is evident from his derivation. Haefeli's model over- or underestimates the average pressure depending on the value of ν and D/H.

For design purposes it may be useful to know the maximum pressure near the centre of the structure. Since the one-dimensional model displays the same functional dependence upon ν and D/H as the finite element calculations, we can adapt the model to calculation of the maximum pressure near the centre of the structure by noting that the calculation for D/H = 0, $\nu = 0.25$ yields a value for C of 1.28. This suggests that if we had chosen a spring constant $k' = \frac{\mu}{D + 0.6H}$, we would be able to match the maximum values. This proves to be the case, as illustrated in Figures 17 and 18. Thus, we could write an expression for the maximum pressure near the centre of the structure as:

$$\bar{\sigma}_{11} = -\left\{\left[\sqrt{\left(\frac{2}{1-\nu}\right)\left(\frac{D}{H} + 0.6\right)}\right] + \frac{\nu}{1-\nu}\frac{\cot \Psi}{2}\right\} \bar{\rho} g H \sin \Psi \qquad (94)$$

Table 1 shows calculated values for the expression in brackets in Equation 94 with the calculated finite element values.

This exercise leaves little doubt of the correctness of the one-dimensional model in terms of dependence on D/H and ν for the linear problem. Of course, the only accurate method to calculate snow pressure is by the two-dimensional numerical method. The advantage of such a model is the physical insight it gives to the problem. Haefeli's equations cannot be derived from continuum mechanics and, furthermore, they contain a questionable dependence upon Poisson's ratio and D/H. In addition, Haefeli's results

Table 1. Comparison of Most Negative Principal Stress near Centre of Structure from Finite Element Calculations with the Predictions of Equation 94 for the Dynamic Component of Pressure C, where C is the Quantity in Brackets in Equation 94

For Figure 17: $\Psi = 45°$; $D/H = 0.2$

ν	C for one-dimensional model	C for finite element calculations
0	1.26	1.28
0.1	1.33	1.34
0.2	1.41	1.42
0.25	1.46	1.47
0.3	1.51	1.53
0.35	1.57	1.62
0.4	1.63	1.74

For Figure 18: $\Psi = 45°$; $\nu = 0.25$

D/H	C for one-dimensional model	C for finite element calculations
0	1.26	1.27
0.2	1.46	1.46
0.5	1.71	1.72
1.0	2.07	2.08
2.0	2.63	2.66
3.0	3.10	3.12

show an angular dependence of $\frac{1}{\cos \Psi}$ for C, which neither finite element calculations (Langdon, 1975) nor the one-dimensional model exhibits.

It should be emphasized that the one-dimensional model is developed for the linear problem. When non-linearity is assumed by making the shear and bulk viscosity proportional to the bulk stress, the pressures will increase over those given by the one-dimensional model. Neither the one-dimensional model nor Haefeli's equations are derived to include such non-linearity. McClung (1976a) showed that bulk stress effects increase the pressures by 20% or more for typically expected values of ν and D/H.

In regard to Haefeli's model the following comments seem in order. His model shows a much stronger Poisson dependence than the one-dimensional model or the finite element calculations and, in fact, his equations are divergent as $\nu \to 0.5$. Haefeli's model also shows much stronger dependence on D/H than either the one-dimensional model or the finite element calculations.

Haefeli's formulation is based on the concept of a back pressure zone or zone of influence of the structure upslope. For the one-dimensional model with an exponential dependence on distance, the back pressure zone is theoretically infinite. We could, however, define such a quantity for our distribution by recognizing that the exponential distribution will return to 99% of the neutral zone value in the distance:

$$x' \simeq 5\sqrt{\frac{HE'}{k'}} \tag{95}$$

from Equation 88. This can be rewritten as:

$$x' \simeq 5H\sqrt{\frac{2}{1-\nu}\left(\frac{D}{H}+\frac{1}{2}\right)} \tag{96}$$

For the calculations in McClung (1976a) for D/H = 0.06, D/H = 0.32, H = 3.54 m, and ν = 0.3, we get respectively x' = 22 m and 27 m in agreement with the reported values of 21 m and 28 m. For most applications, however, it is difficult to define the back pressure zone accurately in numerical schemes because larger elements are normally taken far away from the structure. However, the finite element results indicate that Equation 96 is a good estimate of the back pressure zone length even though the usefulness of this parameter in snow pressure work is questionable.

Figure 19 shows a typical comparison of glide velocity in the back pressure zone from finite element calculations with back pressure zone velocities from the one-dimensional model for D/H = 0.32 and ν = 0.3 for linear constitutive equations for a

slope angle $\Psi = 45°$. This figure illustrates the back pressure zone problem adequately. Calculation of $\frac{x'}{H}$ from Equation 96 yields $\frac{x'}{H} = 7.7$, which is in good agreement with the finite element scheme. Haefeli's expression for the back pressure zone is (Salm, 1977):

$$x_b = \frac{2H}{\cos \Psi} \left[\left(\frac{1-\nu}{1-2\nu} \right) \left(1 + \frac{3D}{H} \right) \right]^{\frac{1}{2}} \tag{97}$$

In the present case, this equation yields:

$$\frac{x_b}{H} = 5.2$$

Haefeli's equations consistently underestimate the back pressure zone estimates when compared with the one-dimensional model or the finite element calculations.

COMMENTS ON SWISS GUIDELINES FOR AVALANCHE DEFENCE

The Swiss Guidelines for avalanche defence (Avalanche Control in the Starting Zone, 1962) are based on Haefeli's formulation of snow pressure. In view of the differences between the formulation of Haefeli and the one-dimensional model, it is instructive to put the one-dimensional model in the same form.

For the one-dimensional model the total force S, parallel to the slope per unit length, would be approximately from Equation 90:

$$S = - \bar{\rho} g H^2 \sin \Psi \left[\sqrt{\left(\frac{2}{1-\nu} \right) \left(\frac{D}{H} + \frac{1}{2} \right)} \right] - \frac{\nu}{1-\nu} \frac{\bar{\rho} g H^2}{2} \cos \Psi \tag{98}$$

The equivalent expression for Haefeli's formulation is (Salm, 1977):

$$S_N = - \bar{\rho} g H^2 \sin \Psi \left[\frac{2}{3} \left(\frac{1-\nu}{1-2\nu} \right)^{\frac{1}{2}} \frac{(1 + 3D/H)^{\frac{1}{2}}}{\cos \Psi} \right] - \frac{\nu}{1-\nu} \frac{\bar{\rho} g H^2}{2} \cos \Psi \tag{99}$$

Comparison of these expressions indicates that the differences lie in the brackets in the first terms. The Swiss guidelines separate the terms in brackets into creep and glide factors. However, the derivation of the one-dimensional model indicates that it is physically clearer to compare the bracketed terms in these two formulations because any "glide factor" will involve coupling of Poisson effects. Division into creep and glide factors can lead to false conclusions about the effect of gliding as does the comparison done by Langdon (1975) as well as formulations by Roch, de Quervain and Figilister in de Quervain and Figilister (1953). From the standpoint of the one-dimensional model, an expression like

$$\sqrt{1 + 2\frac{D}{H}}$$

is *not* strictly a "glide factor," since it represents coupling between creep and glide in the problem. It should also be remarked that since the solutions of Roch and de Quervain are essentially reformulations of Bucher's work (Bucher, 1948), they cannot be correct in any case, since his work contains inconsistencies (Salm, 1977).

BOUNDARY CONDITION EFFECTS FOR SNOW PRESSURE PROBLEMS

When a structure is present on a slope, the snow will compact against the structure by creep and glide and, thus, densify. Experiments providing creep measurements on slopes and on horizontal snow covers indicate that as alpine snow compacts, measured strain-rates are approximately independent of depth in the snow cover. One possible explanation of this is that the shear and bulk viscosity are stress dependent (Mellor, 1968; Brown *et al.*, 1973; McClung, 1975). As discussed previously, this could indicate that the leading terms in the constitutive law are proportional to the bulk stress, σ_{kk}. Now if it is assumed that the creep of snow compacting against a structure is affected in the same way, then the appropriate glide constitutive equation may be of the form (McClung, 1975):

$$\tau = \frac{k\sigma_{kk}}{D} u \qquad (100)$$

if glide is assumed to be by creep.

Thus, for snow pressure problems, the glide constitutive equation should be in general non-linear. This approach disregards the viscosity non-linearity owing to stress conditions over individual asperities, which may be present to a small degree.

When separation occurs, the boundary condition is of the form:

$$\tau = \frac{\mu_w}{L} u \tag{101}$$

and, therefore, in the general case, the boundary condition for snow pressure problems should be non-linear where creep and lubrication sliding are competitive mechanisms.

Behind a structure there will be a distribution of shear stress and glide velocity at the glide interface. In addition, the normal stress can be higher in the back pressure zone. Therefore, the conditions in this non-neutral zone can be less favourable for separation.

For the case in which the interface is of the form of a single sine wave, the separation condition in the neutral zone is:

$$\frac{\langle 2P^2 \rangle^{\frac{1}{2}}}{\sigma - P_w} = \frac{\sqrt{2}}{\pi} \frac{\tan \Psi}{(1-k)} \frac{1}{r} \tag{102}$$

For the non-neutral zone condition, $\sigma - P_w$ can be increased by the presence of a structure as a first approximation. Finite element calculations for linear creep and glide constitutive equations show that initially there is an increase in σ of about 60% immediately behind a structure if slip is permitted along the structure and that it decays exponentially to the neutral zone value.

We can estimate the extra normal stress effects in the back pressure zone in the following manner for the one-dimensional model. If there is no slip on the structure the value of the normal stress, σ_z, will be approximately the neutral zone value. However, if slip is permitted along the structure there will be an added normal stress which can be estimated from equilibrium considerations to be approximately given by:

$$H \frac{\partial \tau}{\partial x}$$

Thus, an approximate estimate of the distribution of normal stress in the back pressure zone is given by:

$$\begin{aligned} \sigma_z &\simeq -\sigma_N = -\bar{\rho} g H \cos \Psi && \text{for no slip on the structure} \\ \sigma_z &\simeq -(\sigma_N + H \frac{\partial \tau}{\partial x}) && \text{for a smooth structure} \end{aligned} \tag{103}$$

For the one-dimensional model this last expression can be written:

$$\sigma_z \simeq -\left(\sigma_N + \tau_g \sqrt{\frac{1-\nu}{2}\frac{1}{\left(\frac{D}{H}+\frac{1}{2}\right)}}\ \exp -\sqrt{\frac{1-\nu}{2\left(\frac{D}{H}+\frac{1}{2}\right)}}\frac{x}{H}\right) \tag{104}$$

For typical parameters with $\Psi = 45°$, this normal stress is on the order of $1.6\ \sigma_N$ near the structure which is potentially important to the question of separation. Two-dimensional finite element calculations attest to the accuracy of this estimate. Langdon (1975) estimates $\sigma_{z(0)} \simeq 1.6\ \sigma_N$ from such calculations. For $\nu = 0.3$, $D/H = 0.32$, the estimate near the structure is $\sigma_{z(0)} \simeq 1.65\ \sigma_N$. This argument should only be taken as very approximate.

Separation depends on the pressure fluctuations at the glide interface and these in turn are proportional to the glide velocity which increases in an exponential manner in the back pressure zone. The presence of a structure might inhibit separation due to compression effects. Since the glide velocity is zero at the structure, fast glide is not possible there. This hypothesis has a potentially important application in formulations of snow pressure problems. Suppression of extensive separation immediately in back of a structure could place an upper limit on the value of the stagnation depth parameter in the immediate vicinity of the structure of less than H, while application of open slope measurements would indicate values up to 3H.

EXTENSION TO LOW SLOPE ANGLES--APPROXIMATE INCLUSION OF SETTLEMENT IN THE ONE-DIMENSIONAL MODEL

The one-dimensional model was derived by assuming that the snowpack deforms in simple shear and does not include settlement effects. For slope angles less than 45°, there can be increased pressure over that predicted by the one-dimensional model owing to interruption of settlement or vertical deformation. The foregoing comparisons indicate that the assumption of simple shear deformation is adequate for slope angles close to 45°. Finite element calculations indicate that both the dynamic pressure and back pressure zone increase over that given by the one-dimensional model for slope angles less than 45°. Settlement effects for low slope angles can be accounted for approximately by decreasing the stiffness for creep in the model as the slope angle decreases from 45°. Therefore, the dynamic component of pressure might be approximated by:

$$\bar{\sigma}_1 \simeq -\sqrt{\left(\frac{2}{1-\nu}\right)\left(\frac{D}{H}+\frac{1}{2}\cot\Psi\right)}\ \bar{\rho} g H \sin\Psi \qquad \text{for } \Psi \leq 45° \tag{105}$$

$$\bar{\sigma}_1 = -\sqrt{\left(\frac{2}{1-\nu}\right)\left(\frac{D}{H}+\frac{1}{2}\right)}\ \bar{\rho} g H \sin\Psi \qquad \text{for } \Psi \geq 45° \tag{106}$$

For $\Psi \leq 45°$, the back pressure zone may be approximated as:

$$x' \simeq 5H\sqrt{\left(\frac{2}{1-\nu}\right)\left(\frac{D}{H}+\frac{1}{2}\cot\Psi\right)} \tag{107}$$

Finite element calculations show that these formulae are accurate in the range of avalanche starting zone slope angles, i.e., down to angles as low as $\Psi = 30°$. Figure 20 shows a comparison for $\Psi = 30°$; $D/H = \frac{1}{2}$; $\nu = 0.25$; $H = 5$ m. Calculation of x' gives 47.8 m, which compares with that of approximately 46 m for the finite element calculations.

From the preceding section we can similarly give formulae representing the maximum *dynamic* pressure for slope angles less than 45° as

$$\sigma_1 = -\sqrt{\left(\frac{2}{1-\nu}\right)\left[\frac{D}{H}+0.6\ (\cot\Psi)\right]}\ \bar{\rho} g H \sin\Psi \tag{108}$$

For the example in Figure 20, this expression gives $\sigma_1/\tau_g = 2.03$, whereas the finite element calculation gives $\sigma_1/\tau_g = 1.98$ for the ratio of most negative principal stress to τ_g near the centre of the structure for an error of 2.5% at $\Psi = 30°$.

Caution should be used in extending the one-dimensional model to very low slope angles because settlement will dominate over shear deformation in such cases and the assumptions will deviate greatly from the original ones. In addition, not much is known about glide on very low slope angles. For a given ground roughness configuration, there may be a threshold shear stress below which glide may not normally occur.

The foregoing argument in regard to settlement effects may be understood by referring to a geometrical argument similar to that introduced by Haefeli (Bader *et al.*, 1939) provided certain restrictions are employed.

Consider a homogeneous, isotropic snowpack deforming linearly in a neutral zone. The shear and vertical stress may then be expressed as:

$$\bar{\sigma}_{xz} = \bar{\rho} g \sin \Psi \, z = \mu \frac{\partial u}{\partial z}$$

$$\bar{\sigma}_{zz} = -\bar{\rho} g \cos \Psi \, z = (2\mu + \lambda) \frac{\partial v}{\partial z} \qquad (109)$$

where μ and λ are the shear viscosity and viscous analog of Lame's constant, respectively. Taking the ratio of these expressions gives (for $z \neq 0$):

$$\tan \Psi = -\left(\frac{\frac{\partial u}{\partial z}}{\frac{\partial v}{\partial z}}\right) \frac{1}{2 + \frac{\lambda}{\mu}} \qquad (110)$$

Using the definition of the deformation-rate coefficient (Perla, 1972) and the viscous analog of Poisson's ratio, this equation may be expressed as:

$$D_i \tan \Psi = \frac{1}{2}\left(\frac{1-2\nu}{1-\nu}\right) \qquad (111)$$

As long as one is far away from boundaries, i.e., the free surface at the top of the snowpack or the restraint condition at the snow-earth interface, D_i, for the present linear problem, admits a simple geometric interpretation defined by Haefeli and emphasized by Perla, namely $D_i = \tan \beta$ where β is the creep angle defined as the ratio of creep velocity components, i.e., $\tan \beta = -\frac{v}{u}$. Substituting this value gives:

$$\tan \beta \tan \Psi = \frac{1}{2}\left(\frac{1-2\nu}{1-\nu}\right) \qquad (112)$$

This equation was introduced by Haefeli and is useful under the assumptions given above. It predicts that the component of shear deformation is greater than the component of settlement deformation for slope angles, $\Psi > 26.6°$ for Poisson ratios greater than 0. For slope angles of 45°, the deformation would be overwhelming in shear. For snow pressure problems, the foregoing finite element analysis proves that the assumption of simple shear deformation is an adequate representation for slope angles near 45°.

The foregoing analysis applied to the one-dimensional model indicates that there will be a Poisson dependence in any real accounting of settlement effects in the

snow pressure problem for slopes of 30° or less. The numerical calculation given here for $\Psi = 30°$, however, shows that the formulae given above are fairly accurate down to $\Psi = 30°$ for $\nu = 0.25$. For lower Poisson ratios the approximation will not be as good for low slope angles. However, a built-in effect supplied by nature on slopes of low angle is expected to help the situation. Simply, this is that densification is greater on less steep slopes such that higher Poisson ratios may be expected on slopes of low angle provided by the settlement effect itself. A more sophisticated approach to the settlement effect will evidently require a two-dimensional treatment. Settlement effects clearly destroy the one-dimensionality of the snow pressure problem.

It should also be noted that the foregoing remarks apply equally well to the case frequently observed in the field in which the components of u and v are linear with depth provided one is far enough away from the free-surface and snow-interface boundaries.

The concept of a creep angle can be a very useful and important quantity in snow mechanics problems if its use is made within the context of the assumptions given above. The creep angle admits definition in terms of internal deformation in a snowpack and therefore measurements of creep angles should be only interpretable provided they are taken in the middle section of a snowpack and for the proper conditions. For example, the creep angle is undefined, in general, at the snow-earth interface. Similarly, field experience shows that the creep components u and v are only linear with depth on slopes of well-settled snow of fairly large depth. It is obvious that u and v could not be linear with depth through the entire snowpack because this would imply that snow at the free surface had sheared under no applied shear stress. Field experience also shows that the deformation components are only linear with depth throughout the midsection of a thick snowpack. As the free surface is approached there is a curving back of the deformation to provide the expected result that the deformation profile meets the free surface at 90°. Generally, at a free surface the neutral zone deformation-rate coefficient is either infinite or undefined and the creep angle also may lose meaning. Therefore, measurements of creep angles or deformation-rate coefficients near the surface of a snowpack may be hard to interpret. The creep angle is intended to represent internal deformation within the snowpack for isotropic, relatively homogeneous snow.

Definition of creep angles or deformation-rate coefficients within thin snowpacks or thin snow slabs suffer from other difficulties of a rather fundamental nature. Thin slabs and snowpacks are often subject to strong temperature gradients and subject to wildly fluctuating temperature conditions. These conditions are known to produce anisotropy in snowpacks by recrystallization. From data on flat study plots it is known that such layers settle very slowly with respect to other layers. It is difficult to apply this result to slopes, but the known strength anisotropy of such

temperature gradient recrystallized snow (relatively weak in shear and strong in compression) coupled with this result may translate to anisotropy in creep deformation, which neither the creep angle nor deformation-rate coefficient is intended to model. It is apparent that such a kind of creep deformation anisotropy could mean that layers of such recrystallized snow would tend to deform relatively easier in shear than if they were isotropic homogeneous snow, so that the estimate of Equation 112 would be conservative. Thus, the component of shear deformation *might* exceed that for settlement deformation for slopes with angles less than 27° for $\nu = 0$ for these kinds of layers.

As long as the discussion above is borne in mind, there is an obvious connection of the predictions of Equation 112 with dry snow slab release. Settlement is generally considered a stable trend in dry snow slab release problems, while shear deformation is thought to promote instability. The majority of slab avalanches occur on slopes greater than 25° and most occur near slope angles approaching 40°. For such slope angles, the component of shear deformation exceeds that for settlement deformation and this discussion may provide a partial explanation of the low number of snow slab releases observed on slopes of low angle. There are, however, many other factors involved.

References

Avalanche Control in the Starting Zone. 1962. Rocky Mountain Forest and Range Experiment Station Paper No. 71, Fort Collins, CO. (Translation of Swiss guidelines by H. Frutiger.)

Bader, H. von, R. Haefeli, E. Bucher, J. Neher, O. Eckel, C. Thams and P. Niggli. 1939. Der schnee und seine metamorphose. Beitr. Geol. Schweiz Geotech. Ser. Hydrologie, No. 3. (English translation: U.S. Snow, Ice and Permafrost Research Establishment. Translation 14, 1954.)

Batchelor, G.K. 1967. *An Introduction to Fluid Dynamics*. Cambridge, England, Cambridge University Press.

Brown, C.B., R.J. Evans and D. McClung. 1973. Incorporation of glide and creep measurements into snow slab mechanics. *In* Symp. on Advances in North American Avalanche Technology, ed. R.I. Perla, 1972. U.S. Dept. of Agriculture Forest Service, General Technical Report RM-3, pp. 7-13.

Bucher, E. 1948. Beitrag zu den theoretischen grundlagen des lawinenverbaus. Beitr. Geol. Schweiz Geotech. Ser. Hydrologie, No. 6.

Cleary, M.P. and J.R. Rice. 1974. Some elementary models for fluid-saturated elastic porous media with compressible constituents. Brown University Report No. MRL E-91.

Domaschuk, L. and N.H. Wade. 1969. A study of bulk and shear moduli in sand. J. Soil Mech. Found. Div. ASCE, 95:561-581.

Dunne, T., A.G. Price and S.C. Colbeck. 1976. The generation of runoff from subarctic snowpacks. Water Resour. Res. 12(4):677-685.

Haefeli, R. 1948. Schnee, lawinen, firn and gletscher. Sonderabdruck aus Ingenieur-Geologie L. Bendel. Vol. II. Springer-Verlag Wien.

Kamb, B. 1970. Sliding motion of glaciers: theory and observations. Rev. Geophys. Space Phys. 8(4):673-728.

Langdon, J.A. 1975. Approximate solutions for the interruption of the creep and glide of snow by avalanche defenses. M.S. Thesis, University of Washington.

McClung, D.M. 1974. Avalanche defense mechanics. Ph.D. Thesis, University of Washington.

McClung, D.M. 1975. Creep and the snow-earth interface condition in the seasonal alpine snowpack. *In* Snow Mechanics, Proc. of the Grindelwald Symp., April 1974. IAHS-AISH Publ. No. 114, pp. 235-248.

McClung, D.M. 1976a. Snow pressure on rigid obstacles. J. Glaciol. 17(76):277-285.

McClung, D.M. 1976b. Laws of friction in snow mechanics. *In* Fjellsprengningsteknikk, Bergmekanikk, Geoteknikk, 1975. Norsk Jord og Fjellteknisk Forbund Tilknyttet NIF, Tapir Press, pp. 26.1-26.6.

McClung, D.M. 1977. Direct simple shear tests on snow and their relation to slab avalanche formation. J. Glaciol. 19(81):101-111.

McClung, D.M. 1979. Shear fracture precipitated by strain softening as a mechanism of dry slab avalanche release. J. Geophys. Res. 84:3519-3526

Mellor, M. 1964. Properties of snow. Cold Regions Science and Engineering Report, Part 3, Section A. U.S. Army Corps Eng. Cold Reg. Res. Eng. Lab., Hanover, New Hampshire.

Mellor, M. 1968. Avalanches. Cold Regions Science and Engineering Monograph, Part III, Section A3, U.S. Army Corps Eng. Cold Reg. Res. Eng. Lab., Hanover, New Hampshire.

Michell, A.G.M. 1950. *Lubrication: Its Principles and Practice*. London and Glasgow: Blackie & Son, Ltd.

Nye, J.F. 1969. A calculation on the sliding of ice over a wavy surface using a Newtonian viscous approximation. Proc. R. Soc. London Ser. A, Vol. 311, pp. 445-467.

Nye, J.F. 1970. Glacier sliding without cavitation in a linear viscous approximation. Proc. R. Soc. London Ser. A, Vol. 315, pp. 381-403.

Palmer, A.C. and J.R. Rice. 1973. The growth of slip surfaces in the progressive failure of over-consolidated clay. Proc. R. Soc. London Ser. A, Vol. 332, pp. 527-548.

Perla, R.I. 1972. Generalization of Haefeli's creep-angle analysis. J. Glaciol. 11(63):447-450.

Perla, R.I. and E.R. LaChapelle. 1970. A theory of snow slab failure. J. Geophys. Res. 75(36):7619-7627.

Quervain, M.R. de and R. Figilister. 1953. Zum schneedruckproblem. Winterbericht des Eidg. Institutes für Schneeund Lawinenforschung, No. 16, pp. 89-98.

Rice, J.R. and M.P. Cleary. 1975. Some basic stress-diffusion solutions for fluid-saturated elastic porous media with compressible constituents. Brown University Report No. NSF GA-43380/4.

Rice, J.R. and D.A. Simons. 1975. The stabilization of spreading shear faults by coupled deformation-diffusion effects in fluid-infiltrated porous materials. Brown University Div. of Eng. Report No. GA-43380/5.

Salm, B. 1967. An attempt to clarify triaxial creep mechanics of snow. *In* Physics of Snow and Ice, ed. Hirobumi Ôura, Int. Conf. Low Temp. Sci. (Sapporo, Japan, August 1966). Proc. Inst. of Low Temp. Sci., Hokkaido University, Vol. I, Pt. 2, pp. 857-874.

Salm, B. 1975. A constitutive equation for creeping snow. *In* Snow Mechanics, Proc. of the Grindelwald Symp., April 1974. IAHS-AISH Publ. No. 114, pp. 222-235.

Salm, B. 1977. Snow forces. J. Glaciol. 19(81):67-100.

Wroth, C.P. 1972. Some aspects of the elastic behaviour of overconsolidated clay. *In* Stress-Strain Behaviour of Soils, ed. R.H.G. Parry, Henley-on-Thames, Foulis, pp. 347-361.

Figures

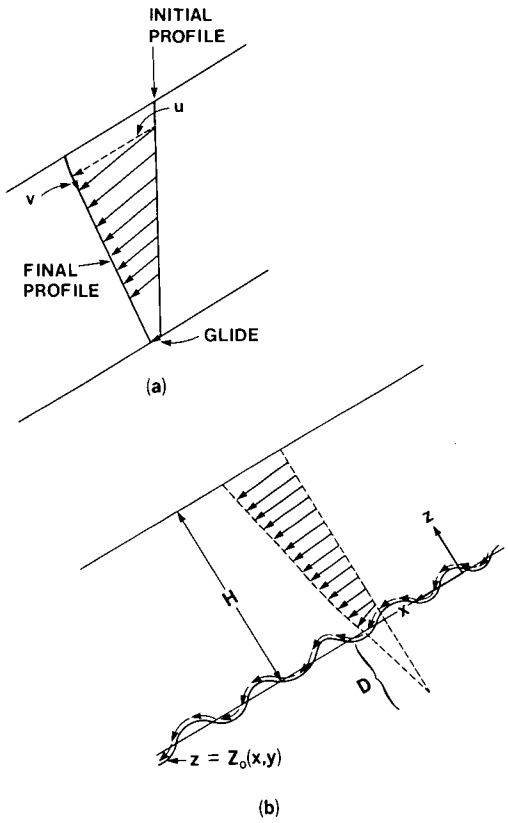

Figure 1. (a) Schematic of typical neutral zone creep and glide data. (b) Schematic of snowpack creeping internally and gliding over an interface with stagnation depth, D, and snowpack depth H.

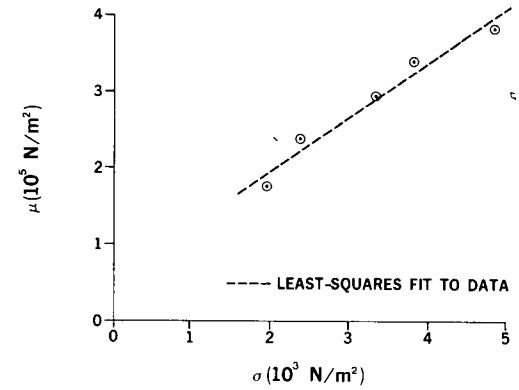

Figure 2. Initial tangent modulus, μ, vs. normal stress, σ, for five similar snow samples in direct simple shear. Average initial density 260 kg/m^3. Sheared at a rate of 0.15 mm/min. Temperature, -7°C.

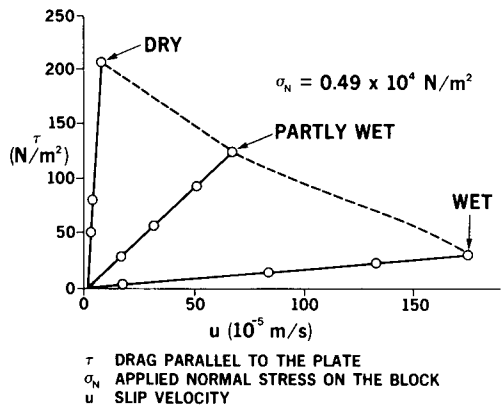

Figure 3. Results of Haefeli's experiments of snow blocks sliding over an inclined glass plate for various degrees of interface wetness.

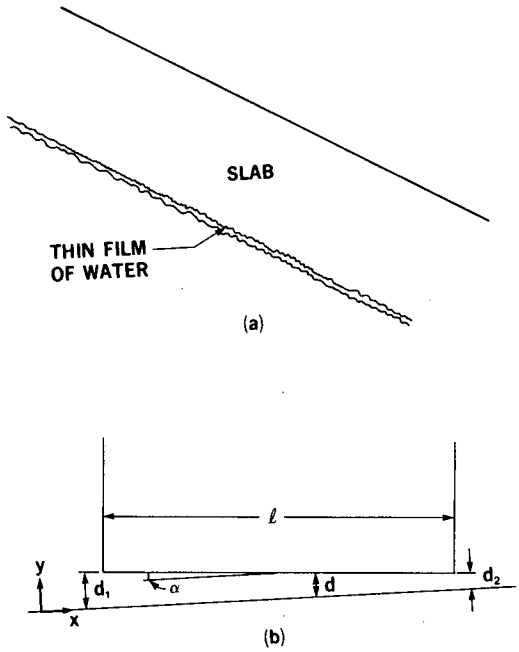

Figure 4. Lubrication sliding mechanism. (a) Slab gliding over thin film. (b) Lubrication layer between plane surfaces after Batchelor (1967).

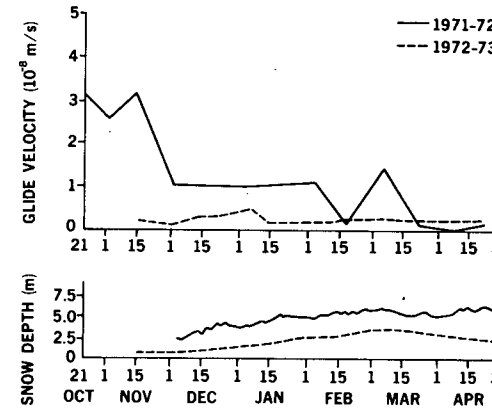

Figure 5. Glide data from a timbered slope showing possible dependence on snow depth. The steady glide during mid-season may be due to suppression of lubrication sliding fluctuations by the trees.

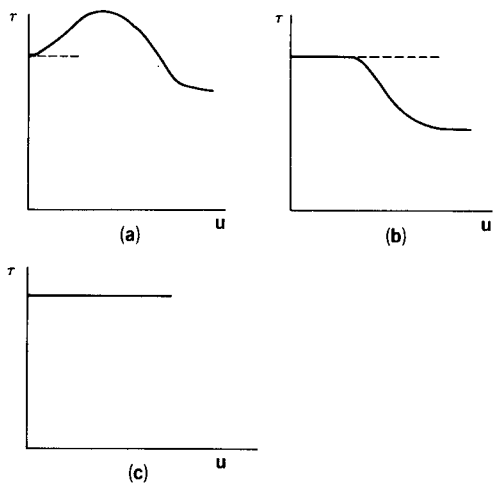

Figure 6. Three possible relationships between shear stress (τ) and glide velocity at the glide interface beneath a snow slab where varying water content or friction conditions are present. (a) and (b) are analogous to strain-softening failures in materials. (c) is a more idealized case analogous to perfect plastic behaviour.

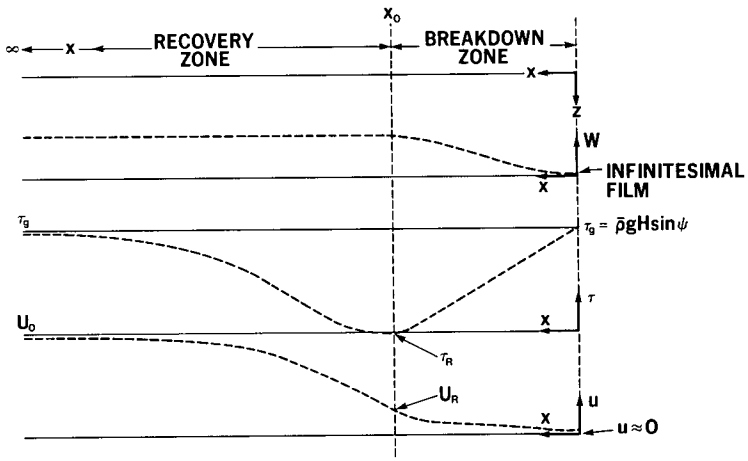

Figure 7. Schematic of water content (w), shear stress (τ), and glide velocity (u) for wet slab conditions vs. distance downslope (x).

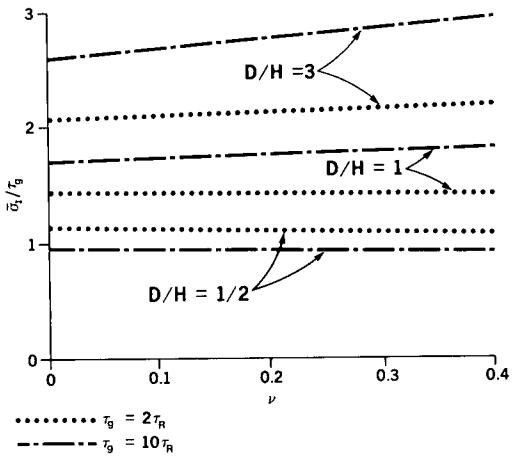

Figure 8. Maximum principal stress $\bar{\sigma}_1$ vs. viscous Poisson's ratio and relative stagnation depth for the one-dimensional model on a 45° slope.

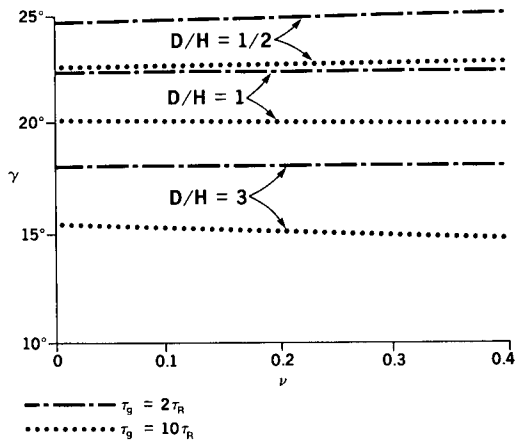

Figure 9. Predictions for the angle (γ) between the glide interface and maximum principal stress vs. viscous Poisson's ratio and relative stagnation depth for a slope angle Ψ = 45°.

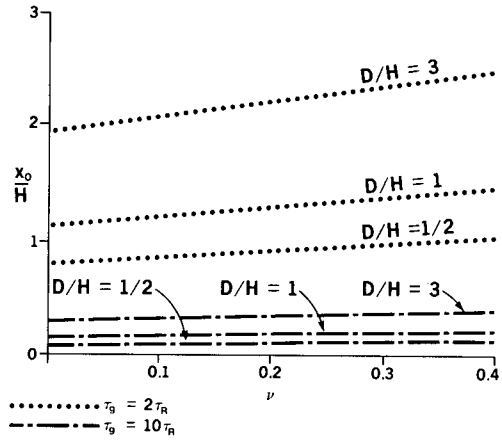

Figure 10. Estimates of breakdown zone length x_0 vs. viscous Poisson's ratio and relative stagnation depth for linear drop in breakdown zone shear stress on a slope of 45°.

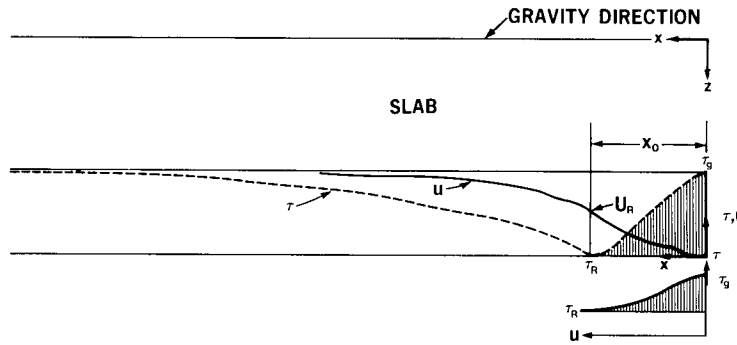

Figure 11. The progressive nature of wet slab avalanche release. The integral of the τ-u relationship in the breakdown zone provides the resistance to expansion of the breakdown zone along the glide interface. This is balanced by the driving force term given in the text.

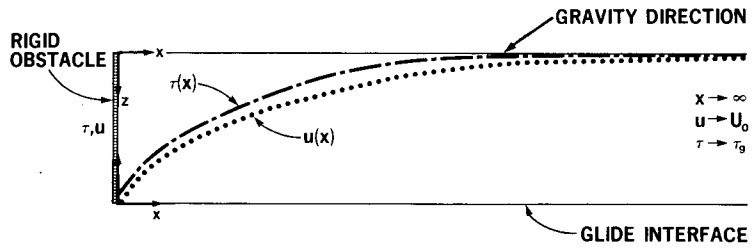

Figure 12. Geometry for one-dimensional snow pressure model. Creep in the snowpack and glide along the interface are interrupted by the presence of a rigid obstacle on the slope.

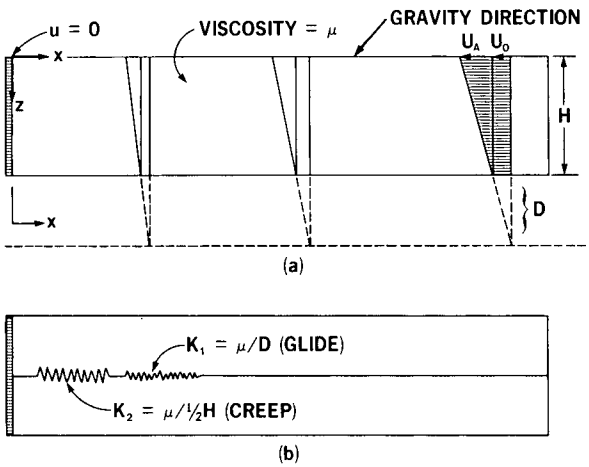

Figure 13. Illustration of (a) one-dimensional snow pressure model and (b) the mechanical spring analogy. $K_2 \to \infty$ for no creep interruption.

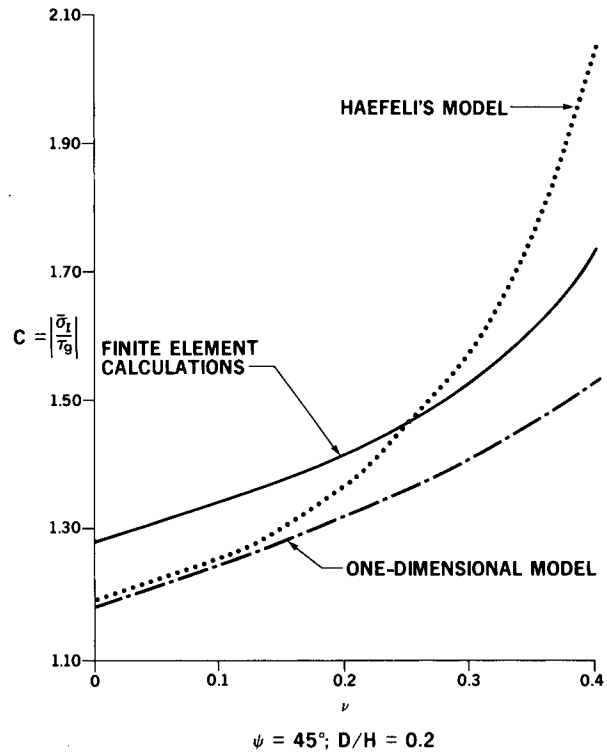

Figure 14. Comparison of dynamic pressure with viscous Poisson's ratio for the one-dimensional model, Haefeli's model, and finite element calculations of most negative principal stress near the structure midpoint, assuming linear creep and glide laws. Static pressure is disregarded.

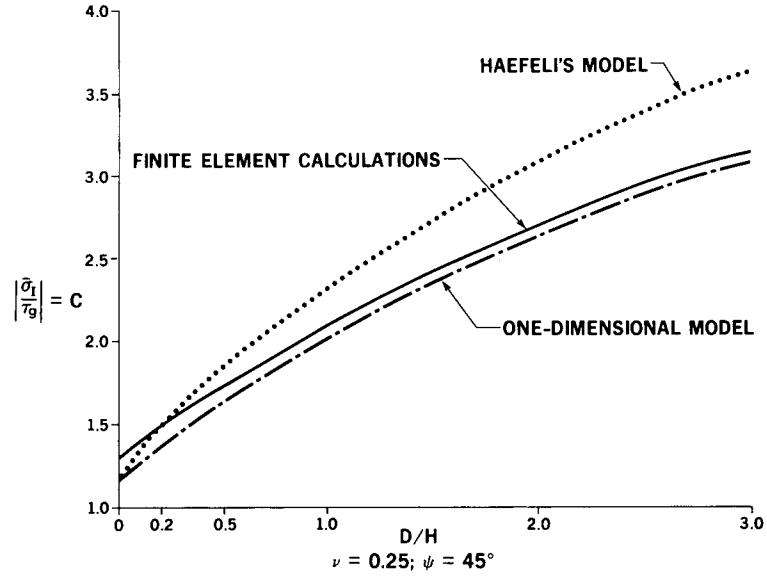

Figure 15. Comparison of ratio of most negative principal stress ÷ τ_g for dynamic pressure as a function of D/H for the one-dimensional model, Haefeli's model, and finite element calculations of the most negative principal stress near the midpoint of the structure for linear creep and glide constitutive equations. Static pressure is disregarded.

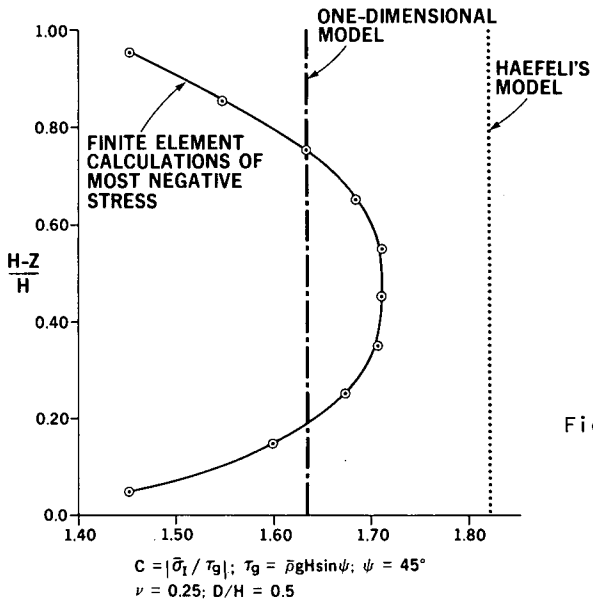

Figure 16. Typical comparison of ratio of dynamic component of pressure to τ_g as a function of relative height on the structure. Linear creep and glide constitutive equations are assumed. Static pressure is disregarded.

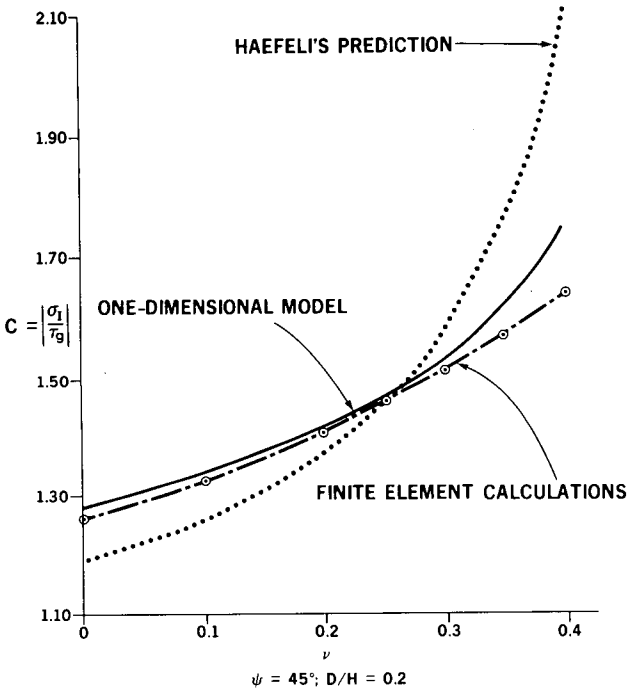

Figure 17. Comparison of most negative principal stress near centre of structure for one-dimensional model from Equation 94 and finite element calculations. Static pressure is disregarded.

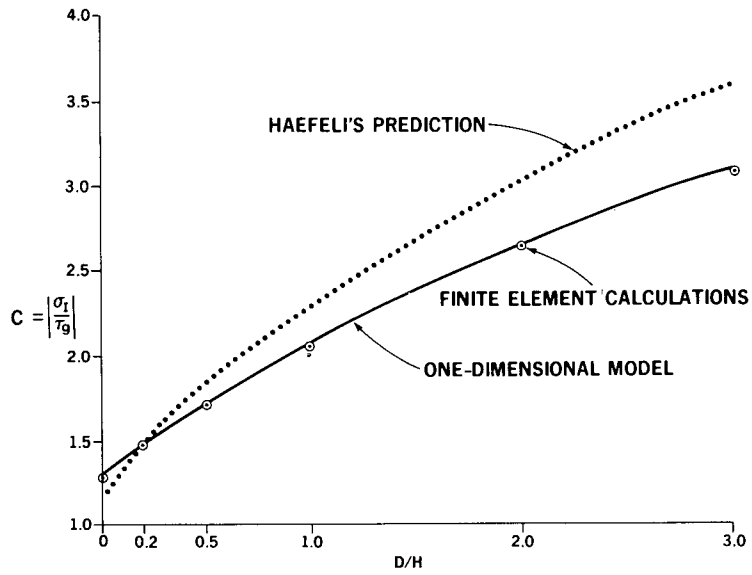

Figure 18. Comparison of most negative principal stress for the one-dimensional model from Equation 94 and finite element calculations near centre of structure for $\nu = 0.25$, $\Psi = 45°$. Static pressure is disregarded.

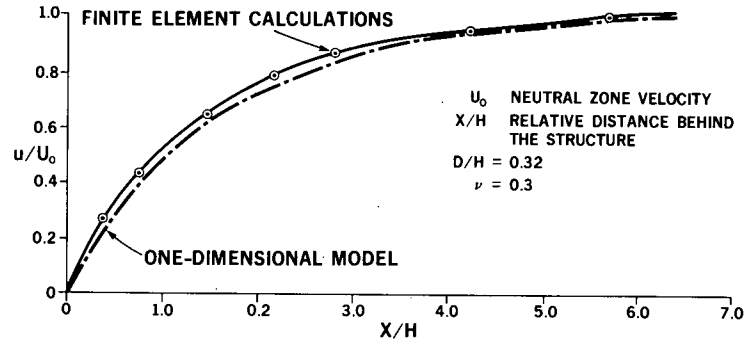

Figure 19. Comparison of glide velocity behind a structure from two-dimensional finite element calculations vs. velocity from the one-dimensional model. Linear constitutive equations.

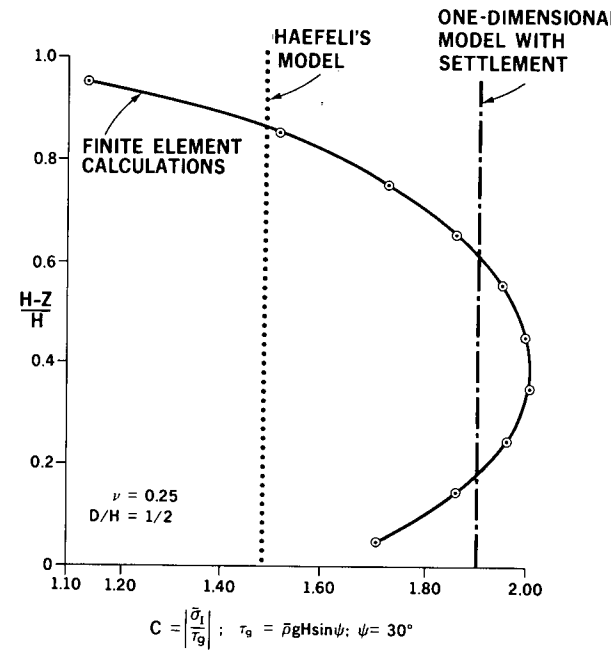

Figure 20. Comparison of dynamic component of pressure for the one-dimensional model with settlement and finite element calculations. Static pressure is disregarded.